

Series Solutions for Orthotropic Diffusion in a Cube

Brian D. Wood**, Sassan Ostvar

*School of Chemical, Biological, and Environmental Engineering, Oregon State University, Corvallis, OR
97330 USA*

Abstract

Analytical solutions to heat or diffusion type equations are numerous, but there are rather few explicit solutions for conditions where the thermal conductivity or diffusion tensors are anisotropic. Such solutions have some use in making predictions for idealization of real systems, but are perhaps most useful for providing benchmark solutions which can be used to validate numerical codes. In this short paper, we present the transient solution to the diffusion equation in a cube under conditions of orthotropic anisotropy in the effective thermal conductivity or diffusion tensor. In particular, we consider the physically-relevant case of transport in a cube with no-flux boundaries for several initial conditions including: (1) a delta function, (2) a truncated Gaussian function, (3) a step function, and (4) a planar function. The potential relevance for each of these initial conditions in the context of validating numerical codes is discussed.

Keywords: , diffusion, thermal transport, analytical solutions, heat equation, diffusion equation

1. Introduction

Diffusive-like processes in anisotropic media has many applications, ranging from heat transport in composite materials [1] to mass and momentum transport in tissues [2]. As a recent topical example, magnetic resonance imaging technologies have been developed to specifically capitalize on the anisotropic structure of neurological tissues; this has lead to a new area of technology known as diffusion tensor imaging (DTI) that has allowed the imaging of neurological tissues at unprecedented levels of detail [3, 4, 5, 6, 7, 8].

Despite the growing interest in diffusive-like processes in anisotropic media, there are very few explicit closed-form solutions available, and fewer that are well-suited for the purposes of testing numerical codes. The frequently referenced compendium of Carslaw and Jaeger [9, §1.17-1.20] discusses the problem of anisotropy at length, but the only explicit solution presented for a rectangular parallelepiped with constant temperature initial conditions and zero temperature boundary conditions [9, §14.5]. Even then, the solution is left in integral

*Corresponding author.

**e-mail address:brian.wood@oregonstate.edu

form, and the coordinate transformation required to achieve a solution is left to the reader to compute.

In this work, we present explicit series solutions for anisotropic heat transport or diffusion in a spatially homogeneous cube for three different initial condition cases. The initial conditions have been selected with the particular purpose of being conditions that are interesting from the perspective of validating numerical codes. Because heat transport and diffusion in a homogeneous anisotropic medium are mathematically identical, the solutions developed in this paper apply to either case. To be specific, note that the diffusion and heat equations are given by

$$\frac{\partial c_{A\gamma}}{\partial t} = \nabla \cdot (\mathbf{D}_\gamma \cdot \nabla c_{A\gamma}) \quad (1)$$

$$\rho c_p \frac{\partial T_{A\gamma}}{\partial t} = \nabla \cdot (\mathbf{K}_\gamma \cdot \nabla T_{A\gamma}) \quad (2)$$

For the case of homogeneous (but anisotropic) systems, we clearly have a correspondence between the diffusion tensor, \mathbf{D}_γ , and the thermal conductivity tensor divided by the product of the density and the heat capacity, $\mathbf{K}_\gamma/(\rho c_p)$. In the remainder of this paper, we will present the solutions for the diffusion equation, with the idea that all of the results are just as applicable to heat transport using the simple correspondence discussed.

In this work, we consider the problem of diffusion of a dilute chemical species in a homogeneous but anisotropic medium, whose diffusion tensor can be expressed by a diagonal tensor with non-equal entries (i.e., an orthotropic tensor). Our intent is to provide new solutions that focus on novel initial value functions; to date, most of the closed-form solutions have been boundary driven. Thus, we have developed solutions for initial conditions that are (1) not constant, and (2) of interest for validation of numerical codes. The novel features of the material presented are primarily the initial conditions covered, and the explicit, closed form of the solutions.

2. Background

For the case of diffusion in isotropic systems, a large number of solutions covering many possible geometries, boundary condition, and initial conditions can be found in the classic texts by Carslaw and Jaeger [9] and Crank [10]. Excellent reviews of more modern papers on this topic can be found in references [11] and [12]. For a particular set of boundary and initial conditions, we follow *explicit* solutions as those which contain only sums and products of well-known solutions (including conventional algebraic, elementary transcendental, and conventional transcendental special functions); following Olver [13], such solutions include infinite series. Series solutions can be very useful when they converge reasonably rapidly because they provide a method to compute high-accuracy approximations to the solution with a finite number of simple computations. Solutions that contain one or more unevaluated integrals are terms *integral* solutions. Although these solutions are also useful, it may not be possible to evaluate the integrals that are encountered in terms of algebraic, transcendental,

or special functions. Such solutions, ultimately, would require a numerical quadrature to evaluate.

Although the literature on the anisotropic case is reasonably well developed, this literature has focussed primarily (although not exclusively) on (1) systems that are orthotropic (i.e., the diffusion tensor is diagonal, but the diagonal entries are not equal), and (2) systems that are driven by boundary conditions rather than initial conditions. The literature for both steady and transient solutions in both 2- and 3- dimensions is summarized in the following paragraphs.

In 2-dimensions, explicit closed-form steady-state solutions have been generated for both the orthotropic case [14, 15], and for the fully anisotropic case [16]. For the 2-dimensional transient case, separation of variables has been successful for developing explicit closed-form solutions for orthotropic cases [17, 18, 19, 20, Ex. 15-6]. The paper by Wang and Chou [21] is unique because it is the only result that allows for general initial conditions; all others have been developed for the zero or (equivalently) constant initial condition. A single paper by Hsieh and Ma [22] reports explicit closed-form results for a fully anisotropic system which are specific to a two-layer infinite slab.

In 3-dimensions, there are explicit closed-form solutions for the steady orthotropic case given by Tungikar and Rao [23], and Hahn and Ozisik [20, Ex. 15-3, 15-4]. Aside from the well-known solution for the infinite domain given by [9], the only other fully transient explicit closed-form solution we were able to find in the literature was the solution of [24] for a finite orthotropic functionally graded plate with zero initial conditions. Although Padovan [25] outlines a variant of the separation of variables approach for a fully anisotropic transient solution, no explicit solutions are provided, and the results are restricted to particular geometries. To date, there appears to be no general approach that yields explicit closed-form solutions for fully anisotropic tensors in which the principle axes are not perpendicular to boundaries of the domain.

Integral solutions (either using Green's functions or Laplace transforms) have also been developed by several researchers for both the orthotropic and the fully anisotropic cases in 2-dimensions [26, 27, 28, 29] and 3-dimensions [30, 31, 32, 33, 34, 35, 36, 37]. These solutions are formally explicit, but they are not in a closed form. Thus, they have the disadvantage of requiring the computation of integrals before an explicit solution can be produced.

3. Symmetry and Positivity of the Diffusion and Thermal Conductivity Tensors

In 1851 George Stokes (of fluid dynamics fame) published a paper arguing that thermal transport was tensorial in nature, and that the associated transport tensor was symmetric. Since that time, there has been substantial discussion on the requirements for the components of a conductivity or diffusion tensor to be physically meaningful (see extensive discussions on the topic in references [38, 39, 40, 41, 42, 38, 43].) The diffusion tensor (or, equivalently, the thermal conductivity tensor) is a positive definite tensor if one accepts the axioms of reciprocity laid out by Onsager [44, 45, 41]. Unlike isotropic tensors, anisotropic tensors have the potential to have zero transport in one or more principle directions, and thus can

only be assured to be positive semidefinite (rather than positive definite). Assuming that the tensor takes the form

$$D_{ij,\gamma} = \begin{bmatrix} a & d & e \\ d & b & f \\ e & f & c \end{bmatrix} \quad (3)$$

then positive semidefiniteness is assured by checking Sylvester's criterion [46] that all of the principal minors are all nonnegative, i.e., $a \geq 0, b \geq 0, c \geq 0, ab - d^2 \geq 0, bc - f^2 \geq 0, ac - e^2 \geq 0$, and $a(bc - f^2) - d(dc - ef) + e(df - be) \geq 0$. At least one of these quantities must be nonzero to prevent the problem from being the trivial case where no transport occurs. Note, however, that it is not necessary that all of the principal minors be nonzero. For example, in a composite medium constructed of impermeable matrix and spanning capillaries aligned in the horizontal plane, the effective diffusion coefficient in the vertical direction is zero, and this would be reflected in the principal minors.

Every three-dimensional second-order positive semidefinite tensor has the following properties: (1) there exist three nonnegative eigenvalues for the tensor; (2) if the three Eigenvalues are distinct and positive, then there exist three unique eigenvectors defining the principal directions of the tensor; (3) these three principle directions are mutually orthogonal, (4) for the case where one or two of the Eigenvalues is zero, or there are positive but repeated Eigenvalues, then there are an infinite number of such mutually orthogonal coordinate systems, and (5) the diffusion tensor is diagonal (but not necessarily isotropic) when expressed in a mutually orthogonal coordinate system constructed from its Eigenvectors. Thus, the anisotropic diffusion equation given by Eqs. (5)-(7) can always be expressed in terms of a orthotropic (diagonal) tensor, \mathbf{D}_γ , when put in the proper mutually-orthogonal coordinate system; the tensor takes the form

$$D_{ij,\gamma} = \begin{bmatrix} D_{xx} & 0 & 0 \\ 0 & \frac{D_{xx}}{d_{yy}^2} & 0 \\ 0 & 0 & \frac{D_{xx}}{d_{zz}^2} \end{bmatrix} \quad (4)$$

Here D_{xx} , D_{yy} , and D_{zz} represent the diffusion coefficients in the direction of the x -, y -, and z -directions, respectively. The other two constants represent the anisotropy in the system, and are defined by $d_{yy}^2 = D_{xx}/D_{yy}$, and $d_{zz}^2 = D_{xx}/D_{zz}$.

For such conditions, the governing differential equation for anisotropic diffusion is well understood. The problem in an *unbounded domain* in 3-dimensions can be stated by

$$\frac{\partial c_{A\gamma}}{\partial t} = \nabla \cdot (\mathbf{D}_\gamma \cdot \nabla c_{A\gamma}) \quad (5)$$

$$\text{Maximum Principle} \quad c(\mathbf{x}, t) \rightarrow 0 \text{ as } \|\mathbf{x}\| \rightarrow \infty \quad (6)$$

Constraint

$$\text{I.C.} \quad c(\mathbf{x}, 0) = \Phi(\mathbf{x}) \quad (7)$$

This problem requires that the initial condition have finite total mass (or energy); in the following we will assume for convenience that the initial condition has a total mass of unity.

The problem diffusive-like transport in an infinite medium was introduced first by Stokes [47]; full solutions to the problem were introduced by Carslaw and Jaeger, although not in explicit form. However, following their discussions in §1.17, §2.2, and §10.2, one can, after a bit of algebra, extract the solutions for the whole space of the form

$$c_{A\gamma}(\mathbf{x}, t) = \frac{1}{2\sqrt{\pi D_{xx}t}} \frac{d_{yy}}{2\sqrt{\pi D_{xx}t}} \frac{d_{zz}}{2\sqrt{\pi D_{xx}t}} \int_{x=-\infty}^{x=\infty} \int_{y=-\infty}^{y=\infty} \int_{z=-\infty}^{z=\infty} \Phi(x', y', z') \exp\left(-\frac{(x-x')^2}{4D_{xx}t}\right) \times \exp\left(-\frac{(y-y')^2 d_{yy}^2}{4D_{xx}t}\right) \exp\left(-\frac{(z-z')^2 d_{zz}^2}{4D_{xx}t}\right) dx' dy' dz' \quad (8)$$

For the initial condition $\Phi(x', y', z') = \delta(x')\delta(y')\delta(z')$ this gives an explicit non-integral solution of the form.

$$c_{A\gamma}(\mathbf{x}, t) = \frac{1}{2\sqrt{\pi D_{xx}t}} \frac{d_{yy}}{2\sqrt{\pi D_{xx}t}} \frac{d_{zz}}{2\sqrt{\pi D_{xx}t}} \exp\left(-\frac{x^2}{4D_{xx}t}\right) \exp\left(-\frac{y^2 d_{yy}^2}{4D_{xx}t}\right) \exp\left(-\frac{z^2 d_{zz}^2}{4D_{xx}t}\right) \quad (9)$$

which is the frequently referenced solution for an instantaneous point source presented by Carslaw and Jaeger [9, §10.2, page 257].

In bounded domains, the variable transformations discussed above can still put the diffusion tensor in orthotropic form; however, the boundary conditions are not, in general, easy to handle (e.g., separable) in this coordinate system. Thus, coordinate transformation does not lead to tractable solutions for the diffusion problem except when the principal axes of the diffusion tensor happen to align with the boundaries of the domain (i.e., the problem is orthotropic because the domain of the parallelepiped is constructed so that the sides aligned with the tensor principle axes.)

Because much of the terminology and early work on this topic came originally from research on the properties of crystals, it is worthwhile to think about an example from a crystal system. A monoclinic crystal is a rhomboid where two of the three planes defining the system are orthogonal, and the third is not. The natural coordinate system describing the geometry of a monoclinic crystal (the crystallographic coordinate system) is one where two of the directional vectors are perpendicular, and the third makes an angle other than 90°. In the natural coordinate system, the thermal conductivity or diffusion tensor can be expressed by the anisotropic tensor [9, §1.17]

$$D_{ij,\gamma} = \begin{bmatrix} a & d & 0 \\ d & b & 0 \\ 0 & 0 & c \end{bmatrix} \quad (10)$$

Although an orthotropic representation of the thermal conductivity or diffusion tensor in such a crystal does have an orthotropic representation in some coordinate system, that

coordinate system is not aligned, in general, with the natural coordinate system of the crystal. Hence, the natural boundaries of the crystal would be complicated functions of more than one variable (and, hence, unlikely to be easily separable), making it difficult to apply separation of variables to the problem directly. This is not a merely academic issue; experimental measurements have been made for diffusion in crystals that show exactly this behavior. A paper by Bendani et al. [48] describes a set of measurements of the diffusion tensor for a naphthalene crystal, and the result is expressed both as an fully anisotropic tensor in the crystallographic coordinate system (i.e., analogous to Eq. (10)), and as an orthotropic tensor (analogous to Eq. 4) when put in the principle axes of the diffusion process.

4. Orthotropic Diffusion in a Cubic Domain

In the remainder of this work, we focus specifically on systems where the coordinate system is organized to yield an is orthotropic diffusion tensor, and the boundary conditions are defined on planes perpendicular to the coordinate axes. We further assume that the domain is a cube with side L ; general rectangular parallelepipeds domains can always be transformed to a cubic domain as described in the Appendix. Although a few solutions do exist in the literature, these solutions have been, to date, either 2-dimensional, or for particularly simple initial and boundary conditions. In this work, we illustrate how the solution can be obtained for arbitrary (assuming only that the function is an admissible one so that the partial differential equation to be well defined) with no-flux conditions at the boundaries. The no-flux conditions correspond closely to conditions that are of interest both for comparison with experimental or numerical results. For this case, the basic mass balance equation and boundary conditions take the form

$$\frac{\partial c_{A\gamma}}{\partial t} = \nabla \cdot (\mathbf{D}_\gamma \cdot \nabla c_{A\gamma}) \quad (11)$$

$$B.C. 1 \quad -\mathbf{n}_\gamma \cdot \mathbf{D}_\gamma \cdot \nabla c_{A\gamma} = 0, \text{ at all boundaries of cube} \quad (12)$$

$$I.C. \quad c(\mathbf{x}, 0) = \Phi(\mathbf{x}) \quad (13)$$

where $\mathbf{L} = (L, L, L)$. Note that in the following, we will assume that \mathbf{D}_γ is a diagonal (but anisotropic) tensor. We will attempt to find a solution using separation of variables. Assume $c_{A\gamma}(x, y, z, t) = T(t)U(x, y, z)$, where $U(x, y, z) = X(x)Y(y)Z(z)$. Substituting this proposed solution yields

$$\frac{\partial T}{\partial t} U = T \mathbf{D}_\gamma : \nabla \nabla U \quad (14)$$

where here $\nabla \nabla U = \frac{\partial^2 U}{\partial x_i \partial x_j}$. Note that because \mathbf{D}_γ is diagonal, we have $\mathbf{D}_\gamma = 0$ for $i \neq j$. Thus, we have

$$\mathbf{D}_\gamma : \nabla \nabla U = D_{ij} \frac{\partial^2 U}{\partial x_j \partial x_i} = D_{xx} \frac{\partial^2 U}{\partial x^2} + D_{yy} \frac{\partial^2 U}{\partial y^2} + D_{zz} \frac{\partial^2 U}{\partial z^2} \quad (15)$$

where each of D_{xx} , D_{yy} , and D_{zz} are (potentially) unique.

4.1. Separation of Variables

For this problem, the process of separation of variables can be used efficiently to develop fully transient, 3-dimensional solutions. Although the approach is reasonably straightforward, the separation does require some careful handling of the separation constants involved. In any event, the separation of this problem does not appear to be well described in the literature. As a result, the process is described in detail in this section.

Using the functional relationship $U(x, y, z) = X(x)Y(y)Z(z)$ and substituting, we find

$$XYZ \frac{\partial T}{\partial t} = YZD_{xx} \frac{\partial^2 X}{\partial x^2} T + XZD_{yy} \frac{\partial^2 Y}{\partial y^2} T + XYD_{zz} \frac{\partial^2 Z}{\partial z^2} T \quad (16)$$

Dividing both sides of this equation by $XYZT$ yields

$$\frac{1}{T} \frac{\partial T}{\partial t} = \frac{D_{xx}}{X} \frac{\partial^2 X}{\partial x^2} + \frac{D_{yy}}{Y} \frac{\partial^2 Y}{\partial y^2} + \frac{D_{zz}}{Z} \frac{\partial^2 Z}{\partial z^2} \quad (17)$$

For later convenience, we normalize this equation by D_{xx} . Defining $d_{yy}^2 = D_{xx}/D_{yy}$ and $d_{zz}^2 = D_{xx}/D_{zz}$, we have

$$\frac{1}{D_{xx}T} \frac{\partial T}{\partial t} = \frac{1}{X} \frac{\partial^2 X}{\partial x^2} + \frac{1}{d_{yy}^2 Y} \frac{\partial^2 Y}{\partial y^2} + \frac{1}{d_{zz}^2 Z} \frac{\partial^2 Z}{\partial z^2} \quad (18)$$

Noting that for this equation, the right-hand side is a function of only X, Y , and Z , and the left-hand side is a function of only T , we conclude, as conventional, that both sides must be equal to a constant. The same argument can be made for each of the terms on the right-hand side independently; each term is independent of all of the others. Thus, we define the separation constant λ^2 by

$$\frac{1}{D_{xx}T} \frac{\partial T}{\partial t} = \frac{1}{X} \frac{\partial^2 X}{\partial x^2} + \frac{1}{d_{yy}^2 Y} \frac{\partial^2 Y}{\partial y^2} + \frac{1}{d_{zz}^2 Z} \frac{\partial^2 Z}{\partial z^2} = -\lambda^2 \quad (19)$$

we note also that, because each of the terms on the right hand side is independent of all others, that each of these terms is also equal to a constant. For convenience, we define these three constants by

$$\lambda^2 = \alpha^2 + \beta^2 + \gamma^2 \quad (20)$$

This defines a set of four ordinary differential equations as follows

$$\frac{dT}{dt} + \lambda^2 D_{xx} T = 0 \quad (21)$$

$$\frac{d^2 X}{dx^2} + \alpha^2 X = 0 \quad (22)$$

$$\frac{d^2 Y}{dy^2} + d_{yy}^2 \beta^2 Y = 0 \quad (23)$$

$$\frac{d^2 Z}{dz^2} + d_{zz}^2 \gamma^2 Z = 0 \quad (24)$$

The solutions to each of these is straightforward. For the time variable, the solution is a decaying exponential of the form

$$T(t) = T_0 \exp(-\lambda^2 D_{xx} t) \quad (25)$$

For the remaining equations, the characteristic equation yields roots of the form $\pm\alpha$, $\pm d_{yy}\beta$, and $\pm d_{zz}\gamma$. Thus, the solutions are trigonometric functions of the form

$$X(x) = A \sin(\alpha x) + B \cos(\alpha x) \quad (26)$$

$$Y(y) = G \sin(d_{yy}\beta y) + H \cos(d_{yy}\beta y) \quad (27)$$

$$Z(z) = R \sin(d_{zz}\gamma z) + S \cos(d_{zz}\gamma z) \quad (28)$$

The use of the no-flux boundary conditions require that these functions obey the relationship

$$X'(x) = \alpha A \cos(\alpha x) - \alpha/L B \sin(\alpha x) \quad (29)$$

$$Y'(y) = d_{yy}\beta G \cos(d_{yy}\beta y) - d_{yy}\beta H \sin(d_{yy}\beta y) \quad (30)$$

$$Z'(z) = d_{zz}\gamma R \cos(d_{zz}\gamma z) - d_{zz}\gamma S \sin(d_{zz}\gamma z) \quad (31)$$

For each of the three boundaries where the origin is included, these relationships indicate that $A = G = R = 0$. Thus the solution is of the form

$$X(x) = B \cos(\alpha x) \quad (32)$$

$$Y(y) = H \cos(d_{yy}\beta y) \quad (33)$$

$$Z(z) = S \cos(d_{zz}\gamma z) \quad (34)$$

The remaining boundary conditions require the following

$$\sin(\alpha L) = 0 \quad (35)$$

$$\sin(d_{yy}\beta L) = 0 \quad (36)$$

$$\sin(d_{zz}\gamma L) = 0 \quad (37)$$

and these are met, respectively, by Eigenvalues of the form $\alpha = \ell\pi/L$, $d_{yy}\beta = m\pi/L$, and $d_{zz}\gamma = n\pi/L$ for $\ell, m, n = 0, 1, 2 \dots$. The solution of the set of differential equations, then, is given by the linear combination of all possible Eigenfunctions.

$$c_{A\gamma}(x, y, z, t) = \sum_{\ell=0}^{\ell=\infty} \sum_{m=0}^{m=\infty} \sum_{n=0}^{n=\infty} \exp(-\lambda^2 D_{xx} t) B_{\ell} H_m S_n \cos(\ell\pi \frac{x}{L}) \cos(m\pi \frac{y}{L}) \cos(n\pi \frac{z}{L}) \quad (38)$$

Recalling the relationship $\lambda^2 = \alpha^2 + \beta^2 + \gamma^2$, then we also have $\lambda^2 = (\ell^2 + m^2/d_{yy}^2 + n^2/d_{zz}^2) \frac{\pi^2}{L^2}$.

$$c_{A\gamma}(x, y, z, t) = \sum_{\ell=0}^{\infty} \sum_{m=0}^{\infty} \sum_{n=0}^{\infty} \exp\left(-\left(\ell^2 + \frac{m^2}{d_{yy}^2} + \frac{n^2}{d_{zz}^2}\right) \frac{\pi^2}{L^2} D_{xx} t\right) \times B_{\ell} H_m S_n \cos(\ell\pi \frac{x}{L}) \cos(m\pi \frac{y}{L}) \cos(n\pi \frac{z}{L}) \quad (39)$$

The constants B_{ℓ} , H_m , and S_n are found in the conventional manner using the initial condition and the orthogonality of the trigonometric functions. Specifically, for $t = 0$ we have

$$\Phi(x, y, z) = \sum_{\ell=0}^{\infty} \sum_{m=0}^{\infty} \sum_{n=0}^{\infty} B_{\ell} H_m S_n \cos(\ell\pi \frac{x}{L}) \cos(m\pi \frac{y}{L}) \cos(n\pi \frac{z}{L}) \quad (40)$$

multiplying both sides of this expression by $\cos(\ell'\pi \frac{x}{L}) \cos(m'\pi \frac{y}{L}) \cos(n'\pi \frac{z}{L})$ and integrating yields

$$\int_{x=0}^{x=L} \int_{y=0}^{y=L} \int_{z=0}^{z=L} \Phi(x, y, z) \cos(\ell'\pi \frac{x}{L}) \cos(m'\pi \frac{y}{L}) \cos(n'\pi \frac{z}{L}) dz dy dx = \sum_{\ell=0}^{\infty} \sum_{m=0}^{\infty} \sum_{n=0}^{\infty} \int_{x=0}^{x=L} \int_{y=0}^{y=L} \int_{z=0}^{z=L} B_{\ell} H_m S_n \cos(\ell\pi \frac{x}{L}) \cos(\ell'\pi \frac{x}{L}) \times \cos(m\pi \frac{y}{L}) \cos(m'\pi \frac{y}{L}) \cos(n\pi \frac{z}{L}) \cos(n'\pi \frac{z}{L}) dz dy dx \quad (41)$$

The right-hand side of this expression is non-zero only for the condition $\ell = \ell'$, $m = m'$, $n = n'$, for which we have

$$\int_{x=0}^{x=L} \int_{y=0}^{y=L} \int_{z=0}^{z=L} \Phi(x, y, z) \cos(\ell\pi \frac{x}{L}) \cos(m\pi \frac{y}{L}) \cos(n\pi \frac{z}{L}) dz dy dx = B_{\ell} H_m S_n \int_{x=0}^{x=L} \int_{y=0}^{y=L} \int_{z=0}^{z=L} \cos^2(\ell\pi \frac{x}{L}) \cos^2(m\pi \frac{y}{L}) \cos^2(n\pi \frac{z}{L}) dz dy dx \quad (42)$$

The trigonometric integral on the right-hand side is easily verified to be $L^3/8$ when $\ell, m, n > 0$. In general, the value of the integral is $L^3/(2^{N_0})$, where N_0 is the number of non-zero indexes (i.e., $N_0 = 0, 1, 2$ or 3). Thus, the value of $B_{\ell} H_m S_n$ is found from

$$B_{\ell} H_m S_n = \frac{2^{N_0}}{L^3} \int_{x=0}^{x=L} \int_{y=0}^{y=L} \int_{z=0}^{z=L} \Phi(x, y, z) \cos(\ell\pi \frac{x}{L}) \cos(m\pi \frac{y}{L}) \cos(n\pi \frac{z}{L}) dz dy dx \quad (43)$$

Note here that the Fourier coefficients are not necessarily independently determinable. For non-separable initial conditions, only the product of the coefficients can be determined;

frequently a single symbol is used for this coefficient (e.g., $\bar{B}_{\ell mn} = B_\ell H_m S_n$). The solution is given by

$$c_{A\gamma}(x, y, z, t) = \sum_{\ell=0}^{\infty} \sum_{m=0}^{\infty} \sum_{n=0}^{\infty} \exp\left(-[\ell^2 \frac{\pi^2}{L^2} D_{xx} + \frac{m^2}{d_{yy}^2} \frac{\pi^2}{L^2} D_{xx} + \frac{n^2}{d_{zz}^2} \frac{\pi^2}{L^2} D_{xx}]t\right) \bar{B}_{\ell mn} \cos(\ell\pi \frac{x}{L}) \cos(m\pi \frac{y}{L}) \cos(n\pi \frac{z}{L}) \quad (44)$$

where the Fourier coefficients are evaluated from

$$\bar{B}_{\ell mn} = \frac{2^{N_0}}{L^3} \int_{x=0}^{x=L} \int_{y=0}^{y=L} \int_{z=0}^{z=L} \Phi(x, y, z) \cos(\ell\pi \frac{x}{L}) \cos(m\pi \frac{y}{L}) \cos(n\pi \frac{z}{L}) dx dy dz \quad (45)$$

For the non-separable initial conditions, it is necessary that the initial condition function be well-behaved enough such that a representation by a triple Fourier series is possible. For the practical purposes discussed here, it is sufficient that the initial condition has meaning in at least a distributional sense.

There is a useful simplification for functions that *are multiplicative* in the form $\Phi(x, y, z) = \Phi_x(x)\Phi_y(y)\Phi_z(z)$ (i.e., *separable*). For this case, we have

$$B_\ell H_m S_n = \frac{2^{N_0}}{L^3} \int_{x=0}^{x=L} \Phi_x(x) \cos(\ell\pi \frac{x}{L}) dx \int_{y=0}^{y=L} \Phi_y(y) \cos(m\pi \frac{y}{L}) dy \int_{z=0}^{z=L} \Phi_z(z) \cos(n\pi \frac{z}{L}) dz \quad (46)$$

and this allows us to determine B_ℓ , H_m , and S_n independently by

$$B_\ell = \frac{2^{N_{0\ell}}}{L} \int_{x=0}^{x=L} \Phi_x(x) \cos(\ell\pi \frac{x}{L}) dx \quad (47)$$

$$H_m = \frac{2^{N_{0m}}}{L} \int_{y=0}^{y=L} \Phi_y(y) \cos(m\pi \frac{y}{L}) dy \quad (48)$$

$$S_n = \frac{2^{N_{0n}}}{L} \int_{z=0}^{z=L} \Phi_z(z) \cos(n\pi \frac{z}{L}) dz \quad (49)$$

where here, $N_{0\ell}$, N_{0m} , and N_{0n} are equal to zero if the associated index (ℓ , m , or n) is zero, and equal to 1 otherwise. For the problems considered here, we have imposed the condition that the total mass in the system is unity; this means that we can compute the zeroth coefficient immediately for the multiplicative initial condition directly by

$$B_0 = \frac{1}{L} \int_{x=0}^{x=L} \int_{y=0}^{y=L} \int_{z=0}^{z=L} \Phi_x(x) dx = \frac{1}{L} \quad (50)$$

$$H_0 = \frac{1}{L} \int_{x=0}^{x=L} \int_{y=0}^{y=L} \int_{z=0}^{z=L} \Phi_y(y) dy = \frac{1}{L} \quad (51)$$

$$S_0 = \frac{1}{L} \int_{x=0}^{x=L} \int_{y=0}^{y=L} \int_{z=0}^{z=L} \Phi_z(z) dz = \frac{1}{L} \quad (52)$$

Because the series involved is a cosine series, it is convenient to make the first term explicit, and represent the remaining terms as a sum from 1 to ∞ . For the multiplicative initial condition, this yields a particularly simple expansion

$$\begin{aligned}
c_{A\gamma}(x, y, z, t) = & \left[B_0 + \sum_{\ell=1}^{\ell=\infty} B_{\ell} \cos(\ell\pi \frac{x}{L}) \exp\left(-\ell^2 \frac{\pi^2}{L^2} D_{xx} t\right) \right] \\
& \times \left[H_0 + \sum_{m=1}^{m=\infty} H_m \cos(m\pi \frac{y}{L}) \exp\left(-\frac{m^2}{d_{yy}^2} \frac{\pi^2}{L^2} D_{xx} t\right) \right] \\
& \times \left[S_0 + \sum_{n=1}^{n=\infty} S_n \cos(n\pi \frac{z}{L}) \exp\left(-\frac{n^2}{d_{zz}^2} \frac{\pi^2}{L^2} D_{xx} t\right) \right] \quad (53)
\end{aligned}$$

4.2. Moments

In applications, it is often desirable to have explicit formulae for the spatial moments of the solution. One reason for this is to provide a global (spatially) measure that can be compared with either experimental data or with numerical results to provide some sense of how much agreement there is with the analytical solution. The zeroth, first, and second moments are usually three that are considered in applications. The zeroth moment (total mass) in each case is normalized to unity. The first moment measures the center of mass of the solution as a function of time, and in the steady state it should be identically equal to $\mathbf{x} = (L/2, L/2, L/2)$ regardless of the initial condition. The second centered moment is particularly useful for diffusion problems, because it relates to the spread of the solution around its first moment.

Zeroth moment

$$m_0(t) = \int_{x=0}^{x=L} \int_{y=0}^{y=L} \int_{z=0}^{z=L} c_{A\gamma}(x, y, z, t) dz dy dx \quad (54)$$

For convenience, the zeroth moment (total mass) for each case is normalized to unity, so that $m_0 = 1$. To obtain a different value for the total mass, m'_0 , one need only multiply the unit mass solution by the appropriate constant so that $c'(x, y, z, t) = m'_0 c(x, y, z, t)$, where $c'(x, y, z, t)$ is the concentration associated with the mass m'_0 .

There are three first moments for the concentration field, one for each of the three Cartesian axes. The first moment is found by evaluating the following integrals.

First moment

$$m_x(t) = \int_{x=0}^{x=L} \int_{y=0}^{y=L} \int_{z=0}^{z=L} x c_{A\gamma}(x, y, z, t) dz dy dx \quad (55)$$

$$m_y(t) = \int_{x=0}^{x=L} \int_{y=0}^{y=L} \int_{z=0}^{z=L} y c_{A\gamma}(x, y, z, t) dz dy dx \quad (56)$$

$$m_z(t) = \int_{x=0}^{x=L} \int_{y=0}^{y=L} \int_{z=0}^{z=L} z c_{A\gamma}(x, y, z, t) dz dy dx \quad (57)$$

For the case of multiplicative initial conditions, the first moments can be computed explicitly by

$$m_x(t) = \frac{L^2}{2} \left[\frac{1}{L} + \frac{2}{\pi^2} \sum_{\ell=1}^{\ell=\infty} B_\ell \frac{(-1 + (-1)^\ell)}{\ell^2} \exp\left(-\ell^2 \frac{\pi^2}{L^2} D_{xx} t\right) \right] \quad (58)$$

$$m_y(t) = \frac{L^2}{2} \left[\frac{1}{L} + \frac{2}{\pi^2} \sum_{m=1}^{m=\infty} H_m \frac{(-1 + (-1)^m)}{m^2} \exp\left(-\frac{m^2}{d_{yy}^2} \frac{\pi^2}{L^2} D_{xx} t\right) \right] \quad (59)$$

$$m_z(t) = \frac{L^2}{2} \left[\frac{1}{L} + \frac{2}{\pi^2} \sum_{n=1}^{n=\infty} S_n \frac{(-1 + (-1)^n)}{n^2} \exp\left(-\frac{n^2}{d_{zz}^2} \frac{\pi^2}{L^2} D_{xx} t\right) \right] \quad (60)$$

For initial conditions that are symmetric about the point $\mathbf{x} = (L/2, L/2, L/2)$ for each of the three coordinate axes, the first moments are by definition $m_x = m_y = m_z = L/2$; thus they do not change in time.

The centered second moments are actually represented by a 3×3 tensor, of the form

$$\mathbf{M} = \begin{bmatrix} M_{xx} & M_{xy} & M_{xz} \\ M_{yx} & M_{yy} & M_{yz} \\ M_{zx} & M_{zy} & M_{zz} \end{bmatrix} \quad (61)$$

In practice, however, it is generally the diagonal elements of the centered moment tensor are of primary interest. The diagonal elements of the centered second moment tensor are given by the following.

Centered second moment

$$M_{xx}(t) = \int_{x=0}^{x=L} \int_{y=0}^{y=L} \int_{z=0}^{z=L} (x - \frac{L}{2})^2 c_{A\gamma}(x, y, z, t) dz dy dx \quad (62)$$

$$M_{yy}(t) = \int_{x=0}^{x=L} \int_{y=0}^{y=L} \int_{z=0}^{z=L} (y - \frac{L}{2})^2 c_{A\gamma}(x, y, z, t) dz dy dx \quad (63)$$

$$M_{zz}(t) = \int_{x=0}^{x=L} \int_{y=0}^{y=L} \int_{z=0}^{z=L} (z - \frac{L}{2})^2 c_{A\gamma}(x, y, z, t) dz dy dx \quad (64)$$

For reference, the off-diagonal elements, $M_{\xi\eta}$, of the centered second moment tensor are defined analogously, e.g.,

$$M_{xy} = \int_{x=0}^{x=L} \int_{y=0}^{y=L} \int_{z=0}^{z=L} (x - \frac{L}{2})(y - \frac{L}{2}) c_{A\gamma}(x, y, z, t) dz dy dx \quad (65)$$

however, the off-diagonal elements will not be considered further here.

For the case of multiplicative initial conditions, an explicit representation of the second moments can be determined by evaluating the integrals above. This leads to the closed-form

expressions

$$M_{xx}(t) = \frac{L^3}{12} \left[\frac{1}{L} + \frac{12}{\pi^2} \sum_{\ell=1}^{\ell=\infty} B_{\ell} \frac{(1 + (-1)^{\ell})}{\ell^2} \exp \left(-\ell^2 \frac{\pi^2}{L^2} D_{xx} t \right) \right] \quad (66)$$

$$M_{yy}(t) = \frac{L^3}{12} \left[\frac{1}{L} + \frac{12}{\pi^2} \sum_{m=1}^{m=\infty} H_m \frac{(1 + (-1)^m)}{m^2} \exp \left(-\frac{m^2}{d_{yy}^2} \frac{\pi^2}{L^2} D_{xx} t \right) \right] \quad (67)$$

$$M_{zz}(t) = \frac{L^3}{12} \left[\frac{1}{L} + \frac{12}{\pi^2} \sum_{n=1}^{n=\infty} S_n \frac{(1 + (-1)^n)}{n^2} \exp \left(-\frac{n^2}{d_{zz}^2} \frac{\pi^2}{L^2} D_{xx} t \right) \right] \quad (68)$$

It is clear from these expressions that at arbitrarily large times, these moments all tend toward the value $L^2/12$, which is the correct value for the centered moment of a uniform cube.

5. Explicit Series Solutions for Particular Initial Conditions

In this section, the series solution for the four initial conditions described previously are computed. The first (when it is different from the value $\frac{L}{2}$) and second moments are also computed as series. To provide a more intuitive feel for the solutions, isosurface plots of the concentration field are presented. For presentation of the plots, we define the diffusive time scales in each of the cardinal directions by

$$T_x^* = \frac{(\frac{L}{2})^2}{D_{xx}} \quad (69)$$

$$T_y^* = \frac{(\frac{L}{2})^2}{d_{yy}^2 D_{xx}} \quad (70)$$

$$T_z^* = \frac{(\frac{L}{2})^2}{d_{zz}^2 D_{xx}} \quad (71)$$

These represent, very approximately, the time it takes for diffusive gradients in the each direction to move a substantial amount of mass to the boundary. Intuitively, gradients in the each direction should approach zero after just a few multiples of the diffusive time scale for that direction. For the plots generated in this work, we will use the set of parameters defined in Table 1; these parameters represent physically reasonable values for diffusion of dilute aqueous species in fluids or gels. For other physical systems (e.g., heat transfer, diffusion in solids), these parameters would obviously have different values. However, there is substantial utility in providing examples that correspond physically to some system, as we have done here. As seen in Table 1, T_x^* is the smallest time scale. Thus, for plotting we have adopted the following normalized time scale

$$t^* = \frac{t}{T_x^*} \quad (72)$$

Table 1: Parameters used in the example computations.

Parameter	Description	Value	Units
L	Domain Size	0.01	[m]
m_0	Total mass of diffusing solute	1.0	$[\mu g]$
$c_\infty = \frac{m_0}{L^3}$	Steady-state solute concentration	1×10^6	$[\mu g/m^3]$
$M_\infty = \frac{L^2}{12}$	Steady-state second moment	8.33×10^{-6}	$[m^2]$
D_{xx}	Diffusion coefficient, x -direction	1×10^{-9}	$[m^2/s]$
d_{yy}^2	Anisotropy ratio, y -direction	2	[-]
d_{zz}^2	Anisotropy ratio, z -direction	4	[-]
T_x^*	Diffusion time scale, x -direction	25000	[s]
T_y^*	Diffusion time scale, y -direction	50000	[s]
T_z^*	Diffusion time scale, z -direction	100000	[s]
a	Size parameter for initial condition, Case 2	$0.5L$	[m]
σ_x	Variance for initial condition, Case 3	$0.1L$	[m]
κ_y	Parameter for planar initial condition, Case 4	20	[-]
κ_z	Parameter for planar initial condition, Case 4	40	[-]

To provide additional confidence in the series solutions have been computed, each using only the first 20 terms of the series, and compared with the results of a previously verified numerical code. The code and convergence is described in detail in §6.

5.1. Case 1

For Case 1, the initial condition is given by the delta function. The delta function provides a good case for assessing how well codes conserve the dependent variable for challenging initial conditions, and are also useful for verifying particle tracking codes [49]. The initial condition for this case is specified by

$$I.C. \quad c(\mathbf{x}, 0) = \delta(\mathbf{x} - \mathbf{L}/2) = \delta(x - L/2)\delta(y - L/2)\delta(z - L/2) \quad (73)$$

The values of the Fourier series constants are found by the conventional arguments using the orthogonality principles of trigonometric series. This evaluation leads to

$$B_0 = H_0 = S_0 = \frac{1}{L} \quad (74)$$

$$B_\ell = \frac{2}{L} \int_0^L \delta(x - L/2) \cos(\ell\pi \frac{x}{L}) dx = \frac{2}{L} \cos(\frac{\ell\pi}{2}), \text{ for } \ell > 0 \quad (75)$$

$$H_m = \frac{2}{L} \int_0^L \delta(y - L/2) \cos(m\pi \frac{y}{L}) dy = \frac{2}{L} \cos(\frac{m\pi}{2}), \text{ for } m > 0 \quad (76)$$

$$S_n = \frac{2}{L} \int_0^L \delta(z - L/2) \cos(n\pi \frac{z}{L}) dz = \frac{2}{L} \cos(\frac{n\pi}{2}), \text{ for } n > 0 \quad (77)$$

Hence, the solution for the concentration field can be given explicitly by

$$\begin{aligned} c_{A\gamma}(x, y, z, t) = & \frac{1}{L^3} \left[1 + 2 \sum_{\ell=1}^{\ell=\infty} \cos(\frac{\ell\pi}{2}) \cos(\ell\pi \frac{x}{L}) \exp\left(-\ell^2 \frac{\pi^2}{L^2} D_{xx} t\right) \right] \\ & \times \left[1 + 2 \sum_{m=1}^{m=\infty} \cos(\frac{m\pi}{2}) \cos(m\pi \frac{y}{L}) \exp\left(-\frac{m^2}{d_{yy}^2} \frac{\pi^2}{L^2} D_{xx} t\right) \right] \\ & \times \left[1 + 2 \sum_{n=1}^{n=\infty} \cos(\frac{n\pi}{2}) \cos(n\pi \frac{z}{L}) \exp\left(-\frac{n^2}{d_{zz}^2} \frac{\pi^2}{L^2} D_{xx} t\right) \right] \end{aligned} \quad (78)$$

Isosurface plots of the normalized concentration appear in Fig. 1.¹

The moments for this solution are found as follows.

Zeroth moment

$$m_0(t) = \int_{x=0}^{x=L} \int_{y=0}^{y=L} \int_{z=0}^{z=L} c_{A\gamma}(x, y, z, t) dz dy dx = 1 \quad (79)$$

First moment

$$m_x(t) = m_y(t) = m_z(t) = \frac{L}{2} \quad (80)$$

The zeroth and first moments are constant for all cases considered, except Case 4 (where the first moment is transient). Where the moments are constant, they are not plotted.

¹Mathematica scripts for computing each of the four concentration field solutions and associated moments as series will be included as ancillary materials in the final submission of this manuscript.

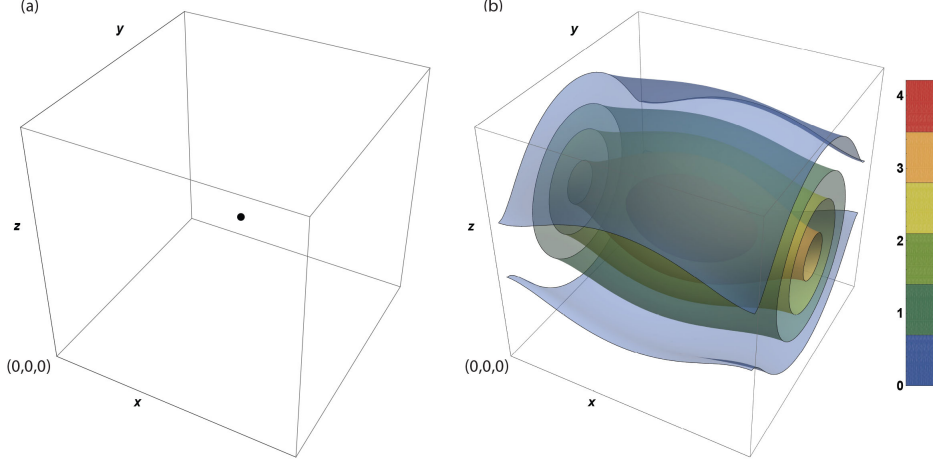


Figure 1: Concentration isosurfaces for the δ -function initial condition (Case 1); concentration is normalized, $\frac{c}{c_\infty}$. (a) Although formally not plottable, the initial condition is represented as a point distribution with finite mass. (b) The concentration field at $t^* = \frac{1}{4}T_x^*$ using the first 20 terms of the series solution.

Centered second moments

$$\begin{aligned}
 M_{xx}(t) &= \int_{x=0}^{x=L} \int_{y=0}^{y=L} \int_{z=0}^{z=L} (x - \frac{L}{2})^2 c_{A\gamma}(x, y, z, t) dz dy dx \\
 &= \frac{L^2}{12} \left[1 + \sum_{\ell=1}^{\ell=\infty} \frac{24}{\ell^2 \pi^2} \exp\left(-\ell^2 \frac{\pi^2}{L^2} D_{xx} t\right) \cos\left(\frac{\ell\pi}{2}\right) (1 + (-1)^\ell) \right] \quad (81)
 \end{aligned}$$

$$\begin{aligned}
 M_{yy}(t) &= \int_{x=0}^{x=L} \int_{y=0}^{y=L} \int_{z=0}^{z=L} (y - \frac{L}{2})^2 c_{A\gamma}(x, y, z, t) dz dy dx \\
 &= \frac{L^2}{12} \left[1 + \sum_{m=1}^{m=\infty} \frac{24}{m^2 \pi^2} \exp\left(-\frac{m^2}{d_{yy}^2} \frac{\pi^2}{L^2} D_{xx} t\right) \cos\left(\frac{m\pi}{2}\right) (1 + (-1)^m) \right] \quad (82)
 \end{aligned}$$

$$\begin{aligned}
 M_{zz}(t) &= \int_{x=0}^{x=L} \int_{y=0}^{y=L} \int_{z=0}^{z=L} (z - \frac{L}{2})^2 c_{A\gamma}(x, y, z, t) dz dy dx \\
 &= \frac{L^2}{12} \left[1 + \sum_{n=1}^{n=\infty} \frac{24}{n^2 \pi^2} \exp\left(-\frac{n^2}{d_{zz}^2} \frac{\pi^2}{L^2} D_{xx} t\right) \cos\left(\frac{n\pi}{2}\right) (1 + (-1)^n) \right] \quad (83)
 \end{aligned}$$

The centered second moments for Case 1 are plotted in Fig. 2. For these plots, we have normalized the moments by their steady-state value, i.e.,

$$M_\infty = \lim_{t \rightarrow \infty} [M_{xx}(t)] = \lim_{t \rightarrow \infty} [M_{yy}(t)] = \lim_{t \rightarrow \infty} [M_{zz}(t)] = \frac{L^2}{12} \quad (84)$$

For plotting purposes, we have defined the following normalized variables

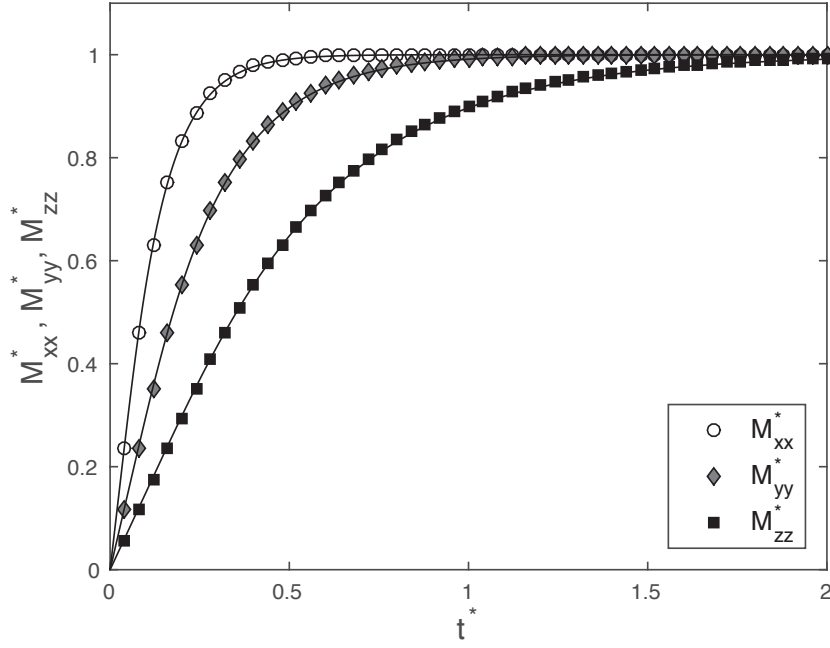


Figure 2: Centered second moments for the δ -function initial condition (Case 1) via series solution (solid lines), and numerical computations (symbols).

$$M_{xx}^* = \frac{M_{xx}}{M_\infty} \quad (85)$$

$$M_{yy}^* = \frac{M_{yy}}{M_\infty} \quad (86)$$

$$M_{zz}^* = \frac{M_{zz}}{M_\infty} \quad (87)$$

5.2. Case 2

For case 2, the initial condition is given by a uniform concentration in a cube of side a centered in the domain. This initial condition poses the typical challenges that discontinuities create in numerical approximation. The solution is also complex enough that it satisfies the guidelines specified by Roache [50] for defining *good* analytical solutions for code verification. To define the initial condition, we first define the following functions in terms of unit Heaviside step functions.

$$\Phi_x(x) = H\left[x - \left(\frac{L}{2} - \frac{a}{2}\right)\right] - H\left[x - \left(\frac{L}{2} + \frac{a}{2}\right)\right] \quad (88)$$

$$\Phi_y(y) = H\left[y - \left(\frac{L}{2} - \frac{a}{2}\right)\right] - H\left[y - \left(\frac{L}{2} + \frac{a}{2}\right)\right] \quad (89)$$

$$\Phi_z(z) = H\left[z - \left(\frac{L}{2} - \frac{a}{2}\right)\right] - H\left[z - \left(\frac{L}{2} + \frac{a}{2}\right)\right] \quad (90)$$

Where $H(x)$ is the unit Heaviside step function. The function, $\Phi(\mathbf{x})$, is given by Defining the function $\Phi(\mathbf{x})$ by

$$\Phi(\mathbf{x}) = \Phi_x(x)\Phi_y(y)\Phi_z(z) \quad (91)$$

The initial condition for a 3-dimensional step function centered in the cubic domain is now specified by

$$I.C. \quad c(\mathbf{x}, 0) = \Phi(\mathbf{x}) \quad (92)$$

The values of the Fourier series constants are found in the conventional manner.

$$B_0 = H_0 = S_0 = \frac{1}{L} \quad (93)$$

$$B_\ell = \frac{2}{L} \int_0^L \Phi(x, y, z) \cos(\ell\pi\frac{x}{L})dx = \frac{4}{L} \int_{\frac{L}{2}-\frac{a}{2}}^{\frac{L}{2}+\frac{a}{2}} \cos(\ell\pi\frac{x}{L})dx = \frac{4 \cos\left(\frac{\pi\ell}{2}\right) \sin\left(\frac{\pi a\ell}{2L}\right)}{\pi a\ell}, \text{ for } \ell > 0 \quad (94)$$

$$H_m = \frac{2}{L} \int_0^L \Phi(x, y, z) \cos(m\pi\frac{y}{L})dy = \frac{2}{L} \int_{\frac{L}{2}-\frac{a}{2}}^{\frac{L}{2}+\frac{a}{2}} \cos(m\pi\frac{y}{L})dy = \frac{4 \cos\left(\frac{\pi m}{2}\right) \sin\left(\frac{\pi a m}{2L}\right)}{\pi a m}, \text{ for } m > 0 \quad (95)$$

$$S_n = \frac{2}{L} \int_0^L \Phi(x, y, z) \cos(n\pi\frac{z}{L})dz = \frac{2}{L} \int_{\frac{L}{2}-\frac{a}{2}}^{\frac{L}{2}+\frac{a}{2}} \cos(n\pi\frac{z}{L})dz = \frac{4 \cos\left(\frac{\pi n}{2}\right) \sin\left(\frac{\pi a n}{2L}\right)}{\pi a n}, \text{ for } n > 0 \quad (96)$$

The explicit series expression for the concentration field is

$$c_{A\gamma}(x, y, z, t) = \frac{1}{L^3} \left[1 + \sum_{\ell=1}^{\ell=\infty} \frac{4L \cos\left(\frac{\pi\ell}{2}\right) \sin\left(\frac{\pi a\ell}{2L}\right)}{\pi a\ell} \cos(\ell\pi\frac{x}{L}) \exp\left(-\ell^2\frac{\pi^2}{L^2}D_{xx}t\right) \right] \times \left[1 + \sum_{m=1}^{m=\infty} \frac{4L \cos\left(\frac{\pi m}{2}\right) \sin\left(\frac{\pi a m}{2L}\right)}{\pi a m} \cos(m\pi\frac{y}{L}) \exp\left(-\frac{m^2}{d_{yy}^2}\frac{\pi^2}{L^2}D_{xx}t\right) \right] \times \left[1 + \sum_{n=1}^{n=\infty} \frac{4L \cos\left(\frac{\pi n}{2}\right) \sin\left(\frac{\pi a n}{2L}\right)}{\pi a n} \cos(n\pi\frac{z}{L}) \exp\left(-\frac{n^2}{d_{zz}^2}\frac{\pi^2}{L^2}D_{xx}t\right) \right] \quad (97)$$

Isosurface plots of the normalized concentration appear in Fig. 3.

The moments for this initial condition are given by the following.

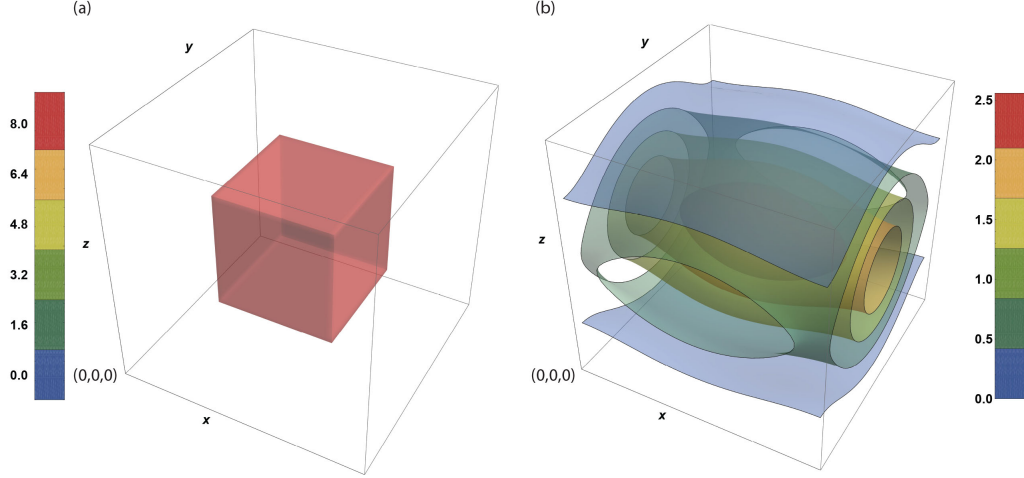


Figure 3: Concentration isosurfaces for the step function initial condition (Case 2); concentration is normalized, $\frac{c}{c_\infty}$. (a) The initial condition. (b) The concentration field at $t^* = \frac{1}{4}T_x^*$ using the first 20 terms of the series solution.

Zeroth moment

$$m_0(t) = \int_{x=0}^{x=L} \int_{y=0}^{y=L} \int_{z=0}^{z=L} c_{A\gamma}(x, y, z, t) dz dy dx = 1 \quad (98)$$

First moment

$$m_x(t) = m_y(t) = m_z(t) = \frac{L}{2} \quad (99)$$

As with Case 1, these moments are constant in time. The centered second moments are, however, transient. Explicit series solutions for these are given by

Centered second moments

$$M_{xx}(t) = \frac{L^2}{12} \left[1 + \frac{12}{\pi^2} \sum_{\ell=1}^{\ell=\infty} \frac{4L \cos\left(\frac{\pi\ell}{2}\right) \sin\left(\frac{\pi a\ell}{2L}\right) (1 + (-1)^\ell)}{\pi a\ell} \frac{1}{\ell^2} \exp\left(-\ell^2 \frac{\pi^2}{L^2} D_{xx} t\right) \right] \quad (100)$$

$$M_{yy}(t) = \frac{L^2}{12} \left[1 + \frac{12}{\pi^2} \sum_{m=1}^{m=\infty} \frac{4L \cos\left(\frac{\pi m}{2}\right) \sin\left(\frac{\pi a m}{2L}\right) (1 + (-1)^m)}{\pi a m} \frac{1}{m^2} \exp\left(-\frac{m^2}{d_{yy}^2} \frac{\pi^2}{L^2} D_{xx} t\right) \right] \quad (101)$$

$$M_{zz}(t) = \frac{L^2}{12} \left[1 + \frac{12}{\pi^2} \sum_{n=1}^{n=\infty} \frac{4L \cos\left(\frac{\pi n}{2}\right) \sin\left(\frac{\pi a n}{2L}\right) (1 + (-1)^n)}{\pi a n} \frac{1}{n^2} \exp\left(-\frac{n^2}{d_{zz}^2} \frac{\pi^2}{L^2} D_{xx} t\right) \right] \quad (102)$$

In Fig. 4, the normalized second moments are plotted as a function of time.

5.3. Case 3

For case 3, the initial condition is given by a truncated Gaussian function. This function is a Gaussian function, centered at $x = y = z = L/2$ which has been truncated at the

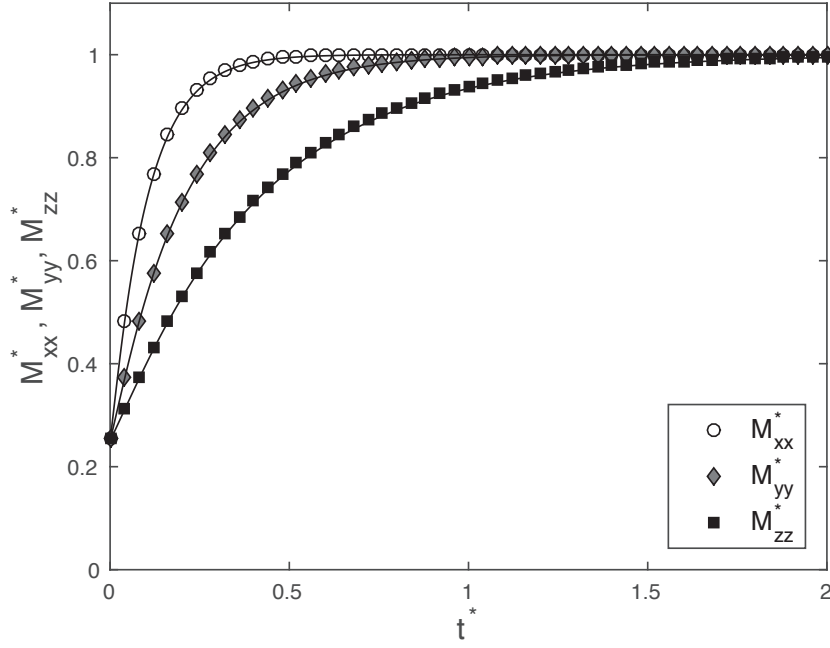


Figure 4: Centered second moments for the step initial condition (Case 2) via series solution (solid lines), and numerical computations (symbols).

boundaries of the domain, and normalized so that the total integrated mass in the domain is unity. Because the function is analytically smooth, numerical approximations to derivatives of it are well-behaved; however, it is complex enough to provide a challenging validation benchmark [50]. This initial condition function is specified explicitly by

$$I.C. \quad c(\mathbf{x}, 0) = \frac{\exp\left(-\frac{(x-\frac{L}{2})^2}{2\sigma_x^2} - \frac{(y-\frac{L}{2})^2}{2\sigma_x^2/d_{yy}^2} - \frac{(z-\frac{L}{2})^2}{2\sigma_x^2/d_{zz}^2}\right)}{\sqrt{2\pi\sigma_x^2}\sqrt{2\pi\sigma_x^2/d_{yy}^2}\sqrt{2\pi\sigma_x^2/d_{zz}^2} \operatorname{erf}\left(\frac{L}{2\sqrt{2}\sigma_x}\right) \operatorname{erf}\left(\frac{L}{2\sqrt{2}(\sigma_x/d_{yy})}\right) \operatorname{erf}\left(\frac{L}{2\sqrt{2}(\sigma_x/d_{zz})}\right)} \quad (103)$$

$$B_0 = H_0 = S_0 = \frac{1}{L} \quad (104)$$

$$B_\ell = \frac{2}{L} \frac{\Re \left[\operatorname{erf} \left(\frac{L^2 + 2i\pi\ell\sigma_x^2}{2\sqrt{2}L\sigma_x} \right) \right]}{\operatorname{erf} \left(\frac{L}{2\sqrt{2}\sigma_x} \right)} \cos \left(\frac{\pi\ell}{2} \right) \exp \left(-\ell^2 \frac{\pi^2}{L^2} \frac{\sigma_x^2}{2} \right), \text{ for } \ell > 0 \quad (105)$$

$$H_m = \frac{2}{L} \frac{\Re \left[\operatorname{erf} \left(\frac{d_{yy}^2 L^2 + 2i\pi m\sigma_x^2}{2\sqrt{2}Ld_{yy}\sigma_x} \right) \right]}{\operatorname{erf} \left(\frac{d_{yy}L}{2\sqrt{2}\sigma_x} \right)} \cos \left(\frac{\pi m}{2} \right) \exp \left(-\frac{m^2}{d_{yy}^2} \frac{\pi^2}{L^2} \frac{\sigma_x^2}{2} \right), \text{ for } m > 0 \quad (106)$$

$$S_n = \frac{2}{L} \frac{\Re \left[\operatorname{erf} \left(\frac{d_{zz}^2 L^2 + 2i\pi n\sigma_x^2}{2\sqrt{2}Ld_{zz}\sigma_x} \right) \right]}{\operatorname{erf} \left(\frac{d_{zz}L}{2\sqrt{2}\sigma_x} \right)} \cos \left(\frac{\pi n}{2} \right) \exp \left(-\frac{n^2}{d_{zz}^2} \frac{\pi^2}{L^2} \frac{\sigma_x^2}{2} \right), \text{ for } n > 0 \quad (107)$$

Note that here at the limit as $\sigma_x \rightarrow 0$, this expression reduces to that for the delta initial condition. Performing the integrations required to evaluate the Fourier coefficients, the closed-form solution for the concentration field is

$$c_{A\gamma}(x, y, z, t) = \quad (108)$$

$$\begin{aligned} & \frac{1}{L^3} \left[1 + \sum_{\ell=1}^{\ell=\infty} 2 \frac{\Re \left[\operatorname{erf} \left(\frac{L^2 + 2i\pi\ell\sigma_x^2}{2\sqrt{2}L\sigma_x} \right) \right]}{\operatorname{erf} \left(\frac{L}{2\sqrt{2}\sigma_x} \right)} \cos \left(\frac{\pi\ell}{2} \right) \exp \left(-\ell^2 \frac{\pi^2}{L^2} \frac{\sigma_x^2}{2} \right) \cos \left(\ell\pi \frac{x}{L} \right) \exp \left(-\ell^2 \frac{\pi^2}{L^2} D_{xx}t \right) \right] \\ & \times \left[1 + \sum_{m=1}^{m=\infty} 2 \frac{\Re \left[\operatorname{erf} \left(\frac{d_{yy}^2 L^2 + 2i\pi m\sigma_x^2}{2\sqrt{2}Ld_{yy}\sigma_x} \right) \right]}{\operatorname{erf} \left(\frac{d_{yy}L}{2\sqrt{2}\sigma_x} \right)} \cos \left(\frac{\pi m}{2} \right) \exp \left(-\frac{m^2}{d_{yy}^2} \frac{\pi^2}{L^2} \frac{\sigma_x^2}{2} \right) \cos \left(m\pi \frac{y}{L} \right) \exp \left(-\frac{m^2}{d_{yy}^2} \frac{\pi^2}{L^2} D_{xx}t \right) \right] \\ & \times \left[1 + \sum_{n=1}^{n=\infty} 2 \frac{\Re \left[\operatorname{erf} \left(\frac{d_{zz}^2 L^2 + 2i\pi n\sigma_x^2}{2\sqrt{2}Ld_{zz}\sigma_x} \right) \right]}{\operatorname{erf} \left(\frac{d_{zz}L}{2\sqrt{2}\sigma_x} \right)} \cos \left(\frac{\pi n}{2} \right) \exp \left(-\frac{n^2}{d_{zz}^2} \frac{\pi^2}{L^2} \frac{\sigma_x^2}{2} \right) \cos \left(n\pi \frac{z}{L} \right) \exp \left(-\frac{n^2}{d_{zz}^2} \frac{\pi^2}{L^2} D_{xx}t \right) \right] \end{aligned} \quad (109)$$

Isosurface plots of the normalized concentration appear in Fig. 5.

The moments for this initial condition are given by the following.

Zeroth moment

$$m_0(t) = \int_{x=0}^{x=L} \int_{y=0}^{y=L} \int_{z=0}^{z=L} c_{A\gamma}(x, y, z, t) dz dy dx = 1 \quad (110)$$

First moment

$$m_x(t) = m_y(t) = m_z(t) = \frac{L}{2} \quad (111)$$

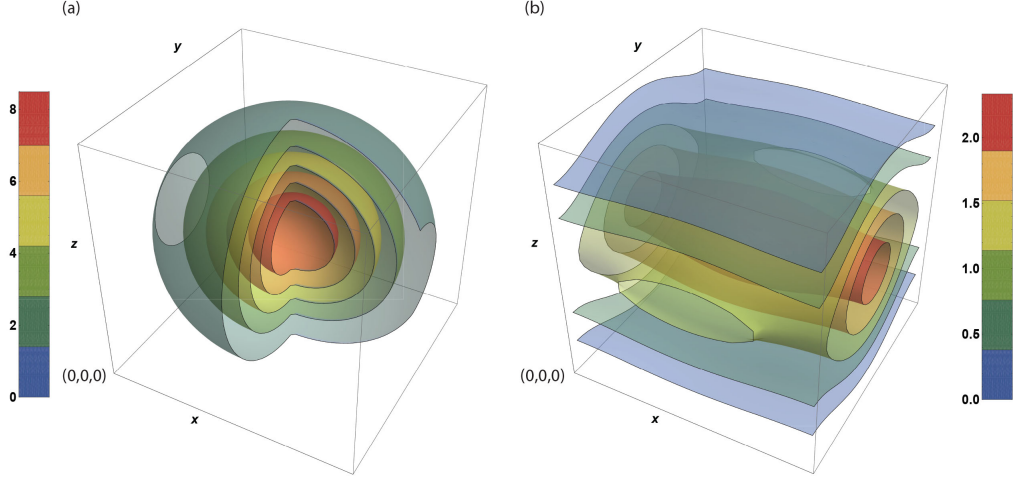


Figure 5: Concentration isosurfaces for the truncated Gaussian initial condition (Case 3); concentration is normalized, $\frac{c}{c_\infty}$. (a) The initial condition. (b) The concentration field at $t^* = \frac{1}{4}T_x^*$ using the first 20 terms of the series solution.

As before, the first two moments are constant in time. The centered second moments are transient, and specified by

Centered second moments

$$M_{xx}(t) = \frac{L^2}{12} \left[1 + \frac{24}{\pi^2} \sum_{\ell=1}^{\ell=\infty} \frac{\Re \left[\operatorname{erf} \left(\frac{L^2 + 2i\pi\ell\sigma_x^2}{2\sqrt{2}L\sigma_x} \right) \right]}{\operatorname{erf} \left(\frac{L}{2\sqrt{2}\sigma_x} \right)} \cos \left(\frac{\pi\ell}{2} \right) \right. \\ \left. \times \exp \left(-\ell^2 \frac{\pi^2}{L^2} \frac{\sigma_x^2}{2} \right) \frac{(1 + (-1)^\ell)}{\ell^2} \exp \left(-\ell^2 \frac{\pi^2}{L^2} D_{xx}t \right) \right] \quad (112)$$

$$M_{yy}(t) = \frac{L^2}{12} \left[1 + \frac{24}{\pi^2} \sum_{m=1}^{m=\infty} \frac{\Re \left[\operatorname{erf} \left(\frac{d_{yy}^2 L^2 + 2i\pi m\sigma_x^2}{2\sqrt{2}Ld_{yy}\sigma_x} \right) \right]}{\operatorname{erf} \left(\frac{d_{yy}L}{2\sqrt{2}\sigma_x} \right)} \cos \left(\frac{\pi m}{2} \right) \right. \\ \left. \times \exp \left(-\frac{m^2}{d_{yy}^2} \frac{\pi^2}{L^2} \frac{\sigma_x^2}{2} \right) \frac{(1 + (-1)^m)}{m^2} \exp \left(-\frac{m^2}{d_{yy}^2} \frac{\pi^2}{L^2} D_{xx}t \right) \right] \quad (113)$$

$$M_{zz}(t) = \frac{L^2}{12} \left[1 + \frac{24}{\pi^2} \sum_{n=1}^{n=\infty} \frac{\Re \left[\operatorname{erf} \left(\frac{d_{zz}^2 L^2 + 2i\pi n\sigma_x^2}{2\sqrt{2}Ld_{zz}\sigma_x} \right) \right]}{\operatorname{erf} \left(\frac{d_{zz}L}{2\sqrt{2}\sigma_x} \right)} \cos \left(\frac{\pi n}{2} \right) \right. \\ \left. \times \exp \left(-\frac{n^2}{d_{zz}^2} \frac{\pi^2}{L^2} \frac{\sigma_x^2}{2} \right) \frac{(1 + (-1)^n)}{n^2} \exp \left(-\frac{n^2}{d_{zz}^2} \frac{\pi^2}{L^2} D_{xx}t \right) \right] \quad (114)$$

The normalized centered second moments are plotted for reference in Fig. 6.

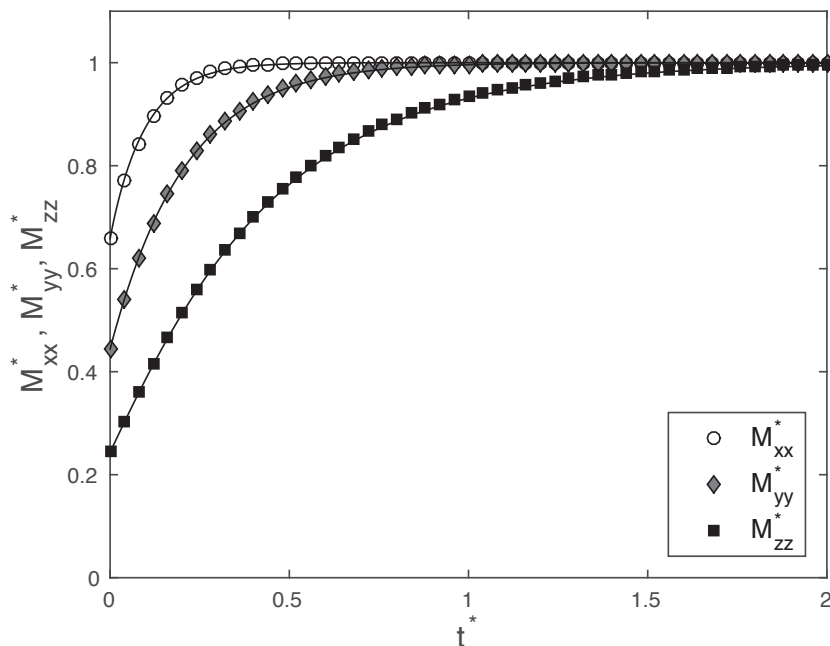


Figure 6: Centered second moments for the truncated Gaussian initial condition (Case 3) via series solution (solid lines), and numerical computations (symbols).

5.4. Case 4

The initial condition for Case 4 was selected specifically because it is not symmetric about the center of the domain. Thus, the center of mass for the solution moves as a function of time. Case 4 would be useful, for example, to provide a solution that would detect canceling errors in a code; symmetric initial conditions may miss such errors because of the symmetry imposed. This case is also the only example provided in this paper for a non-multiplicative form for the initial condition. Other non-multiplicative forms can be handled similarly. To begin, we specify an initial condition that is a plane, given by

$$I.C. \quad c(\mathbf{x}, 0) = \frac{2}{L^4(1 + \kappa_y + \kappa_z)}(x + \kappa_y y + \kappa_z z) \quad (115)$$

Where κ is a parameter that increases the slope of the plane along the z -axis. As with the previous initial conditions, for convenience the total mass for this function is normalized to unity. Unlike previous cases, the evaluation of the Fourier coefficients are not simplified by separability. Coefficients are computed by evaluating the integral given by Eq. (45). Explicitly, this is

$$\bar{B}_{\ell mn} = \frac{2}{L^4(2+a)} \frac{2^{N_0}}{L^3} \int_{x=0}^{x=L} \int_{y=0}^{y=L} \int_{z=0}^{z=L} (x + \kappa_y y + \kappa_z z) \cos(\ell \pi \frac{x}{L}) \cos(m \pi \frac{y}{L}) \cos(n \pi \frac{z}{L}) dx dy dz \quad (116)$$

where $\ell, m, n = 0, 1, 2, \dots$. A simple integration shows that $\bar{B}_{\ell mn}$ is zero when any two of the indexes are greater than zero. Thus, the only non-zero contributions for the coefficients are of the form $B_{\ell 00}$, B_{0m0} , and B_{00n} . This yields

$$\bar{B}_{\ell 00} = \frac{2^{N_0+1}}{L^5(1 + \kappa_y + \kappa_z)} \int_{x=0}^{x=L} x \cos(\ell\pi \frac{x}{L}) dx = \begin{cases} \frac{1}{(1+\kappa_y+\kappa_z)} \frac{4(-1+(-1)^\ell)}{\ell^2\pi^2} \frac{1}{L^3}, & \text{for } \ell > 0 \\ \frac{1}{(1+\kappa_y+\kappa_z)} \frac{1}{L^3}, & \text{for } \ell = 0 \end{cases} \quad (117)$$

$$\bar{B}_{0m0} = \frac{2^{N_0+1}}{L^5(1 + \kappa_y + \kappa_z)} \int_{y=0}^{y=L} \kappa_y y \cos(m\pi \frac{y}{L}) dy = \begin{cases} \frac{\kappa_y}{(1+\kappa_y+\kappa_z)} \frac{4(-1+(-1)^m)}{m^2\pi^2} \frac{1}{L^3}, & \text{for } m > 0 \\ \frac{\kappa_y}{(1+\kappa_y+\kappa_z)} \frac{1}{L^3}, & \text{for } m = 0 \end{cases} \quad (118)$$

$$\bar{B}_{00n} = \frac{2^{N_0+1}}{L^5(1 + \kappa_y + \kappa_z)} \int_{z=0}^{z=L} \kappa_z z \cos(n\pi \frac{z}{L}) dz = \begin{cases} \frac{\kappa_z}{(1+\kappa_y+\kappa_z)} \frac{4\kappa(-1+(-1)^n)}{n^2\pi^2} \frac{1}{L^3}, & \text{for } n > 0 \\ \frac{\kappa_z}{(1+\kappa_y+\kappa_z)} \frac{1}{L^3}, & \text{for } n = 0 \end{cases} \quad (119)$$

Recall, the general solution for the non-multiplicative case is given by Eq. (44); upon substitution, this yields

$$\begin{aligned} c_{A\gamma}(x, y, z, t) = & \frac{1}{L^3} \left[1 + \frac{1}{(1 + \kappa_y + \kappa_z)} \sum_{\ell=1}^{\ell=\infty} \exp\left(-\ell^2 \frac{\pi^2}{L^2} D_{xx} t\right) \frac{4(-1 + (-1)^\ell)}{\ell^2 \pi^2} \cos(\ell\pi \frac{x}{L}) \right. \\ & + \frac{\kappa_y}{(1 + \kappa_y + \kappa_z)} \sum_{m=1}^{m=\infty} \exp\left(-\frac{m^2}{d_{yy}^2} \frac{\pi^2}{L^2} D_{xx} t\right) \frac{4(-1 + (-1)^m)}{m^2 \pi^2} \cos(m\pi \frac{y}{L}) \\ & \left. + \frac{\kappa_z}{(1 + \kappa_y + \kappa_z)} \sum_{n=1}^{n=\infty} \exp\left(-\frac{n^2}{d_{zz}^2} \frac{\pi^2}{L^2} D_{xx} t\right) \frac{4(-1 + (-1)^n)}{n^2 \pi^2} \cos(n\pi \frac{y}{L}) \right] \quad (120) \end{aligned}$$

Note that here, we combined the constant term outside the sum to be consistent with the final form of the previous solutions. As a comment, also note that this problem is the superposition of the three analogous problems in 1-dimension. This is to be expected because of the linearity of the diffusion equation, the boundary conditions, and the initial condition. If the initial condition had not been linear, superposition would not have been possible, and the result would have been much more complex. Isosurface plots of the normalized concentration appear in Fig. 7.

The moments for this initial condition are given by the following.

Zeroth moment

$$m_0(t) = \int_{x=0}^{x=L} \int_{y=0}^{y=L} \int_{z=0}^{z=L} c_{A\gamma}(x, y, z, t) dz dy dx = 1 \quad (121)$$

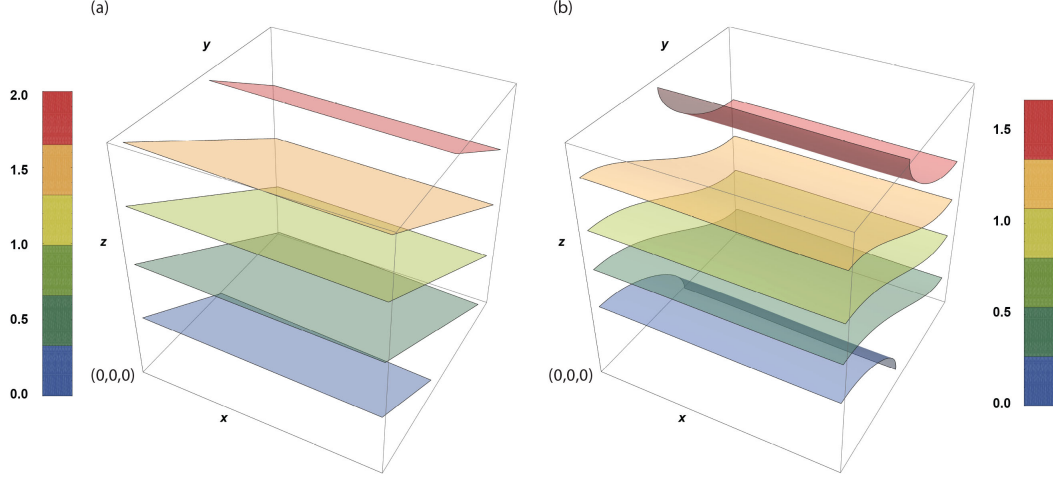


Figure 7: Concentration isosurfaces for the truncated Gaussian initial condition (Case 3); concentration is normalized, $\frac{c}{c_\infty}$. (a) The initial condition. (b) The concentration field at $t^* = \frac{1}{4}T_x^*$ using the first 20 terms of the series solution.

First moments Unlike the previous cases, the first moments for this initial condition are not constant. Integrating Eq. (120) directly (via Eqs. (55)-(57)), the first moments are given by

$$m_x(t) = \frac{L}{2} \left[1 + \frac{1}{(1 + \kappa_y + \kappa_z)} \sum_{\ell=1}^{\ell=\infty} \exp\left(-\ell^2 \frac{\pi^2}{L^2} D_{xx} t\right) \frac{8(-1 + (-1)^\ell)^2}{\ell^4 \pi^4} \right] \quad (122)$$

$$m_y(t) = \frac{L}{2} \left[1 + \frac{\kappa_y}{(1 + \kappa_y + \kappa_z)} \sum_{m=1}^{m=\infty} \exp\left(-\frac{m^2}{d_{yy}^2} \frac{\pi^2}{L^2} D_{xx} t\right) \frac{8(-1 + (-1)^m)^2}{m^4 \pi^4} \right] \quad (123)$$

$$m_z(t) = \frac{L}{2} \left[1 + \frac{\kappa_z}{(1 + \kappa_y + \kappa_z)} \sum_{n=1}^{n=\infty} \exp\left(-\frac{n^2}{d_{zz}^2} \frac{\pi^2}{L^2} D_{xx} t\right) \frac{8(-1 + (-1)^n)^2}{n^4 \pi^4} \right] \quad (124)$$

The first moments in this case are different from the first three cases because the center of mass of the initial condition is different from the center of mass of the steady-state condition; thus, the first moments evolves in time. A plot of the first moments as a function of time is provided in Fig. 8. Note for this plot, we have defined the dimensionless variables

$$m_x^* = \frac{m_x}{L} \quad (125)$$

$$m_y^* = \frac{m_y}{L} \quad (126)$$

$$m_z^* = \frac{m_z}{L} \quad (127)$$

For this case, the centered second moments are complicated by the transient first moments

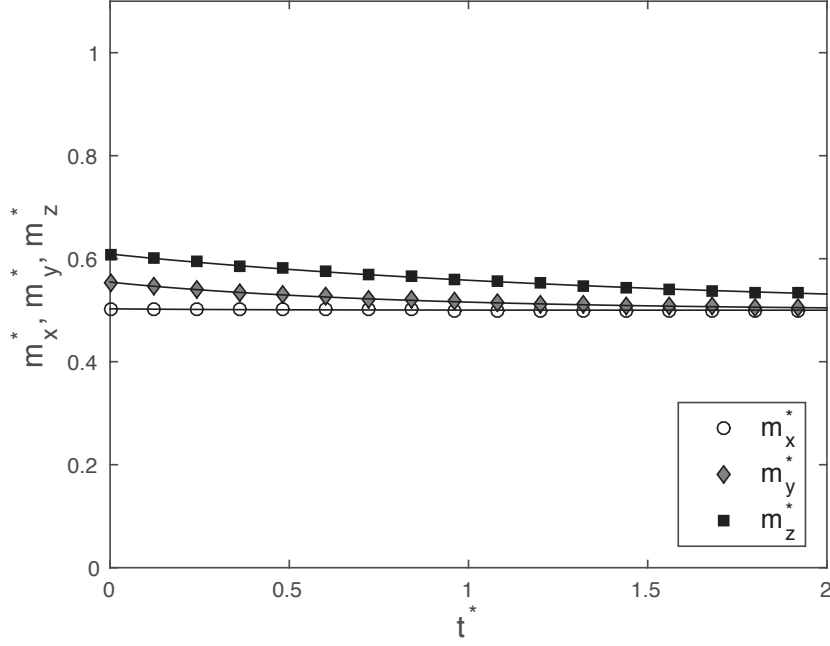


Figure 8: First moments for the plane initial condition (Case 4) via series solution (solid lines), and numerical computations (symbols).

$$M_{xx}(t) = \int_{x=0}^{x=L} \int_{y=0}^{y=L} \int_{z=0}^{z=L} (x - m_x(t))^2 c_{A\gamma}(x, y, z, t) dz dy dx \quad (128)$$

$$M_{yy}(t) = \int_{x=0}^{x=L} \int_{y=0}^{y=L} \int_{z=0}^{z=L} (y - m_y(t))^2 c_{A\gamma}(x, y, z, t) dz dy dx \quad (129)$$

$$M_{zz}(t) = \int_{x=0}^{x=L} \int_{y=0}^{y=L} \int_{z=0}^{z=L} (z - m_z(t))^2 c_{A\gamma}(x, y, z, t) dz dy dx \quad (130)$$

Substituting Eqs. (120) and (122)-(122) into Eqs. (128)-(128), the closed-form expressions for the centered second moment are

Centered second moments

$$\begin{aligned} M_{xx}(t) &= \frac{L^2}{3} - Lm_x(t) + m_x^2(t) \\ &+ \frac{1}{(1 + \kappa_y + \kappa_z)} L^2 \sum_{\ell=1}^{\ell=\infty} \exp\left(-\ell^2 \frac{\pi^2}{L^2} D_{xx} t\right) \frac{8(-1 + (-1)^\ell)}{\ell^4 \pi^4} (-1)^\ell \\ &- \frac{1}{(1 + \kappa_y + \kappa_z)} Lm_x(t) \sum_{\ell=1}^{\ell=\infty} \exp\left(-\ell^2 \frac{\pi^2}{L^2} D_{xx} t\right) \frac{8(-1 + (-1)^\ell)^2}{\ell^4 \pi^4} \end{aligned} \quad (131)$$

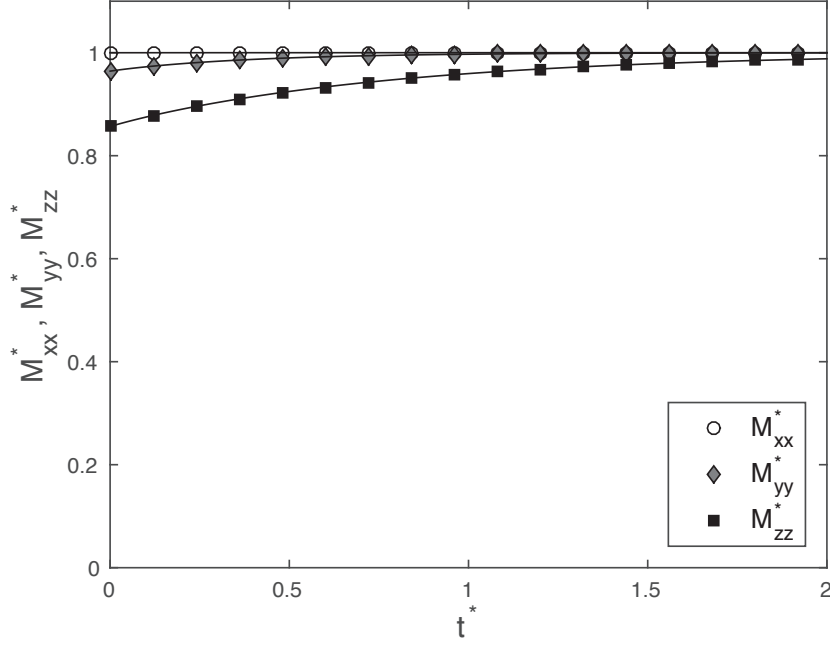


Figure 9: Centered second moments for the plane initial condition (Case 4) via series solution (solid lines), and numerical computations (symbols).

$$\begin{aligned}
M_{yy}(t) &= \frac{L^2}{3} - Lm_y(t) + m_y^2(t) \\
&+ \frac{\kappa_y}{(1 + \kappa_y + \kappa_z)} L^2 \sum_{m=1}^{m=\infty} \exp\left(-\frac{m^2 \pi^2}{d_{yy}^2} \frac{\pi^2}{L^2} D_{xx} t\right) \frac{8(-1 + (-1)^m)}{m^4 \pi^4} (-1)^m \\
&- \frac{\kappa_y}{(1 + \kappa_y + \kappa_z)} Lm_y(t) \sum_{m=1}^{m=\infty} \exp\left(-\frac{m^2 \pi^2}{d_{yy}^2} \frac{\pi^2}{L^2} D_{xx} t\right) \frac{8(-1 + (-1)^m)^2}{\ell^4 \pi^4} \quad (132)
\end{aligned}$$

$$\begin{aligned}
M_{zz}(t) &= \frac{L^2}{3} - Lm_z(t) + m_z^2(t) \\
&+ \frac{\kappa_z}{(1 + \kappa_y + \kappa_z)} L^2 \sum_{n=1}^{n=\infty} \exp\left(-\frac{n^2 \pi^2}{d_{zz}^2} \frac{\pi^2}{L^2} D_{xx} t\right) \frac{8(-1 + (-1)^n)}{n^4 \pi^4} (-1)^n \\
&- \frac{\kappa_z}{(1 + \kappa_y + \kappa_z)} Lm_x(t) \sum_{n=1}^{n=\infty} \exp\left(-\frac{n^2 \pi^2}{d_{zz}^2} \frac{\pi^2}{L^2} D_{xx} t\right) \frac{8(-1 + (-1)^n)^2}{n^4 \pi^4} \quad (133)
\end{aligned}$$

As a check on this result, one can observe that as time becomes arbitrarily large, each of m_x , m_y , and m_z tend toward the value $L/2$. Thus, each of the second centered moments tend to the value $\frac{L^2}{3} - \frac{L^2}{2} + \frac{L^2}{4} = \frac{L^2}{12}$, which is the correct value for the steady-state centered second moment. A plot of the centered second moments appear in Fig. 9.

6. Computations

To demonstrate the utility of the analytical solutions, we conducted direct numerical simulations of diffusion in a cube for a prescribed anisotropic effective diffusivity tensor under the four different initial conditions using the finite element method (FEM) as coded in the commercial package COMSOL Multiphysics 4.4. This code has been previously verified to be a correct FEM representation of the diffusion/heat equations (e.g., [49]), in the sense of Roache [51]. For the simulations in this paper, the parameters summarized in Table 1 were adopted. The code COMSOL solves the discretized equations using the generalized minimal residual method with geometric multigrid preconditioning. Successive over-relaxation was used in pre- and post-smoothing. To assure that the numerical results were converged, the domain was tessellated using a tetrahedral mesh at three levels of refinement.

We use the Grid Convergence Index (GCI) as proposed by Roache [52] to estimate the discretization uncertainties. The GCI is very closely based on Richardson extrapolation and has been developed to serve as an uncertainty and convergence analysis tool in computational fluid dynamics when analytical solutions are not available. The basic idea is to obtain the solution for a given variable ϕ on (at least) three grids with spacings Δ_1 , Δ_2 , and Δ_3 , for which the refinement ratios $r_{21} = \Delta_2 / \Delta_1$, and $r_{32} = \Delta_3 / \Delta_2$, and the variations $\epsilon_{32}(\mathbf{x}) = \phi_3(\mathbf{x}) - \phi_2(\mathbf{x})$, and $\epsilon_{21}(\mathbf{x}) = \phi_2(\mathbf{x}) - \phi_1(\mathbf{x})$ are calculated for values of the fine and medium grid solutions (ϕ_1 and ϕ_2) interpolated on the coarse grid. A *local* (i.e. pointwise) order of accuracy $\mathcal{P}(\mathbf{x})$ can be obtained by solving the following equations iteratively [53]:

$$\mathcal{P}(\mathbf{x}) = \frac{1}{\ln(r_{21})} \left| \ln \left| \frac{\epsilon_{32}(\mathbf{x})}{\epsilon_{21}(\mathbf{x})} \right| + \ln \left(\frac{r_{21}^{\mathcal{P}(\mathbf{x})} - s(\mathbf{x})}{r_{32}^{\mathcal{P}(\mathbf{x})} - s(\mathbf{x})} \right) \right| \quad (134)$$

$$s(\mathbf{x}) = \begin{cases} +1, & \text{if } \epsilon_{32}(\mathbf{x}) \epsilon_{21}(\mathbf{x}) > 0 \\ -1, & \text{if } \epsilon_{32}(\mathbf{x}) \epsilon_{21}(\mathbf{x}) < 0 \end{cases} \quad (135)$$

The fine-grid convergence index is then computed using:

$$\text{GCI}_{fine}^{21} = \frac{1.25 e_a^{21}}{r_{21}^{\mathcal{P}} - 1}, \quad (136)$$

where $e_a^{21} = |(\phi_1 - \phi_2) / \phi_1|$.

Equation (136) can be used to estimate the discretization uncertainty locally or globally. \mathcal{P} and GCI_{fine}^{21} acquire single values for a global variable (e.g. total mass). When local uncertainty estimates are desired, the GCI can be computed locally using a global average of \mathcal{P} [53] as demonstrated in Fig. 10. Based on these, the numerical uncertainties in the fine-grid solutions for the total mass, m_0 , were 0.62%, 0.56%, and 2.06% for the δ -function, Gaussian, and step function cases, respectively (data not shown). We define the percentage

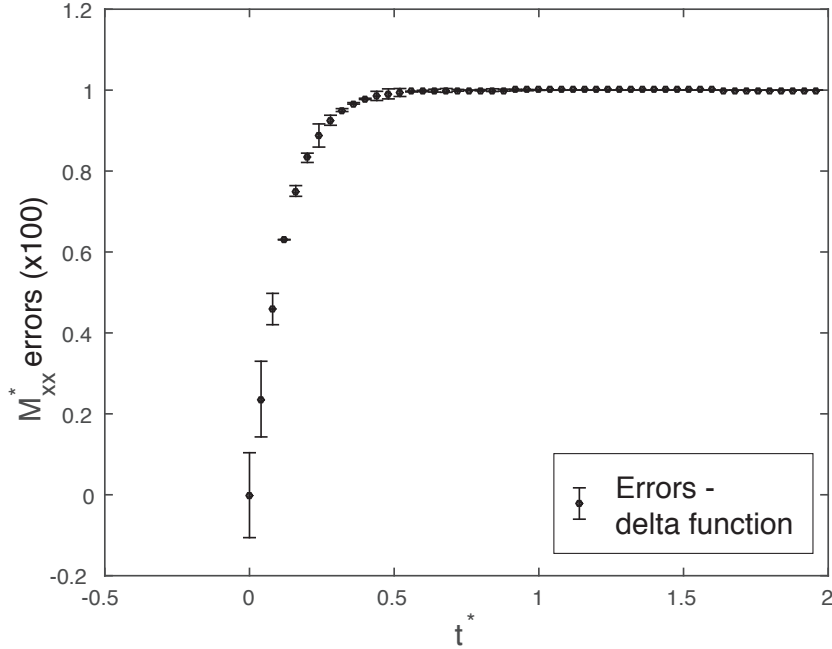


Figure 10: Sample discretization uncertainty estimates for M_{xx} for the δ -function initial condition; the other three initial conditions exhibited similar local errors. Error bars have been magnified 100x to facilitate inspection.

local discretization uncertainty for the second moment by

$$\mu_2 = \frac{GCI_{fine}^{21}}{M_\infty} \times 100 \quad (137)$$

where in this case GCI_{fine}^{21} is the value obtained for computed time point for applicable second moment, M_{xx} , M_{yy} , or, M_{zz} . For all for cases the maximum value of μ_2 for all three moments was less than 10%.

Acknowledgements

This work was supported in part by the National Science Foundation, under grant CBET-336983.

A. Appendix

In this appendix, we briefly explain the transformation of variables required for orthotropic heat or diffusion problems in a rectangular parallelepiped. Coordinate vectors in this system are specified by $\bar{\mathbf{x}} = (\bar{x}, \bar{y}, \bar{z})$, and the parallelepiped has sides of length L in the \bar{x} -direction, and $L_{\bar{y}}$, and $L_{\bar{z}}$ the the other two perpendicular directions. For this case, the problem is specified by

$$\frac{\partial c_{A\gamma}}{\partial t} = D_{\bar{x}\bar{x}} \frac{\partial^2 c_{A\gamma}}{\partial \bar{x}^2} + D_{\bar{y}\bar{y}} \frac{\partial^2 c_{A\gamma}}{\partial \bar{y}^2} + D_{\bar{z}\bar{z}} \frac{\partial^2 c_{A\gamma}}{\partial \bar{z}^2} \quad (\text{A.1})$$

$$B.C. \ 1 \quad -\mathbf{n}_\gamma \cdot \mathbf{D}_\gamma \cdot \nabla c_{A\gamma} = 0, \quad \begin{cases} \text{at all boundaries} \\ \text{of the rectangular} \\ \text{parallelepiped} \end{cases} \quad (\text{A.2})$$

$$I.C. \quad c(\bar{\mathbf{x}}, 0) = \bar{\Phi}(\bar{x}, \bar{y}, \bar{z}) \quad (\text{A.3})$$

Now, define the new variables

$$x = \bar{x} \quad (\text{A.4})$$

$$y = \bar{y} \frac{L_{\bar{y}}}{L} \quad (\text{A.5})$$

$$z = \bar{z} \frac{L_{\bar{z}}}{L} \quad (\text{A.6})$$

From these definitions, it is clear that coordinate vectors (x, y, z) span $(0, 0, 0)$ to (L, L, L) as the coordinate vectors $(\bar{x}, \bar{y}, \bar{z})$ span $(0, 0, 0)$ to $(L, L_{\bar{y}}, L_{\bar{z}})$.

Applying the chain rule twice, it is easy to determine the relationships

$$\frac{\partial^2 c_{A\gamma}}{\partial^2 \bar{x}} = \frac{\partial^2 c_{A\gamma}}{\partial x^2} \quad (\text{A.7})$$

$$\frac{\partial^2 c_{A\gamma}}{\partial^2 \bar{y}} = \frac{L^2}{L_{\bar{y}}^2} \frac{\partial^2 c_{A\gamma}}{\partial y^2} \quad (\text{A.8})$$

$$\frac{\partial^2 c_{A\gamma}}{\partial^2 \bar{z}} = \frac{L^2}{L_{\bar{z}}^2} \frac{\partial^2 c_{A\gamma}}{\partial z^2} \quad (\text{A.9})$$

Finally, denoting

$$D_{xx} = D_{\bar{x}\bar{x}} \quad (\text{A.10})$$

$$D_{yy} = D_{\bar{y}\bar{y}} \frac{L^2}{L_{\bar{y}}^2} \quad (\text{A.11})$$

$$D_{zz} = D_{\bar{z}\bar{z}} \frac{L^2}{L_{\bar{z}}^2} \quad (\text{A.12})$$

$$(\text{A.13})$$

we see that the the final form of the governing equation, boundary conditions, and initial conditions takes the form

$$\frac{\partial c_{A\gamma}}{\partial t} = D_{xx} \frac{\partial^2 c_{A\gamma}}{\partial x^2} + D_{yy} \frac{\partial^2 c_{A\gamma}}{\partial y^2} + D_{zz} \frac{\partial^2 c_{A\gamma}}{\partial z^2} \quad (\text{A.14})$$

$$\text{B.C. 1} \quad -\mathbf{n}_\gamma \cdot \mathbf{D}_\gamma \cdot \nabla c_{A\gamma} = 0, \quad \begin{array}{l} \text{at all boundaries} \\ \text{of the cube} \end{array} \quad (\text{A.15})$$

$$\text{I.C.} \quad c(\mathbf{x}, 0) = \Phi(x, y, z) \quad (\text{A.16})$$

where $\Phi(x, y, z) = \bar{\Phi}(x, \frac{L}{L_y}y, \frac{L}{L_z}z)$ represents the initial condition in the new coordinate system. This problem is identical to that in the main body of the paper, establishing that for all problems on rectangular parallelepiped, there is an equivalent problems for a cubic domain.

References

- [1] J. E. Fischer, W. Zhou, J. Vavro, M. C. Llaguno, C. Guthy, R. Haggenueller, M. Casavant, D. Walters, R. E. Smalley, Magnetically aligned single wall carbon nanotube films: Preferred orientation and anisotropic transport properties, *Journal of applied physics* 93 (4) (2003) 2157–2163.
- [2] A.-R. Khaled, K. Vafai, The role of porous media in modeling flow and heat transfer in biological tissues, *International Journal of Heat and Mass Transfer* 46 (26) (2003) 4989–5003.
- [3] P. J. Basser, Inferring microstructural features and the physiological state of tissues from diffusion-weighted images, *NMR in Biomedicine* 8 (7) (1995) 333–344.
- [4] P. J. Basser, C. Pierpaoli, Microstructural and physiological features of tissues elucidated by quantitative-diffusion-tensor MRI, *Journal of magnetic resonance* 213 (2) (2011) 560–570.
- [5] P. J. Basser, J. Mattiello, D. LeBihan, MR diffusion tensor spectroscopy and imaging., *Biophysical journal* 66 (1) (1994) 259.
- [6] P. J. Basser, J. Mattiello, D. LeBihan, Estimation of the effective self-diffusion tensor from the NMR spin echo, *Journal of Magnetic Resonance, Series B* 103 (3) (1994) 247–254.
- [7] C.-F. Westin, S. E. Maier, H. Mamata, A. Nabavi, F. A. Jolesz, R. Kikinis, Processing and visualization for diffusion tensor MRI, *Medical image analysis* 6 (2) (2002) 93–108.
- [8] C.-F. Westin, S. E. Maier, B. Khidhir, P. Everett, F. A. Jolesz, R. Kikinis, Image processing for diffusion tensor magnetic resonance imaging, in: *Medical Image Computing and Computer-Assisted Intervention—MICCAI’99*, Springer, 441–452, 1999.

- [9] H. S. Carslaw, J. C. Jaeger, *Conduction of heat in solids*, Oxford University (Clarendon) Press, Oxford, second edn., 1959.
- [10] J. Crank, *The Mathematics of Diffusion*– 2nd ed., Oxford University Press, 1975.
- [11] F. De Monte, Unsteady heat conduction in two-dimensional two slab-shaped regions. Exact closed-form solution and results, *International Journal of Heat and Mass Transfer* 46 (8) (2003) 1455–1469.
- [12] X. Lu, P. Tervola, M. Viljanen, A new analytical method to solve the heat equation for a multi-dimensional composite slab, *Journal of Physics A: Mathematical and General* 38 (13) (2005) 2873.
- [13] P. J. Olver, *Introduction to Partial Differential Equations*, S. Axler, K. Ribet, Eds. Undergraduate Texts in Mathematics, Springer, 2014.
- [14] A. Aköz, T. Tauchert, Thermoelastic analysis of a finite orthotropic slab, *Journal of Mechanical Engineering Science* 20 (2) (1978) 65–71.
- [15] T. Tauchert, A. Y. Aköz, Thermal stresses in an orthotropic elastic slab due to prescribed surface temperatures, *Journal of Applied Mechanics* 41 (1) (1974) 222–228.
- [16] C.-C. Ma, S.-W. Chang, Analytical exact solutions of heat conduction problems for anisotropic multi-layered media, *International journal of heat and mass transfer* 47 (8) (2004) 1643–1655, ISSN 0017-9310.
- [17] Y. Sugano, Transient thermal stresses in an orthotropic finite rectangular plate due to arbitrary surface heat-generations, *Nuclear Engineering and Design* 59 (2) (1980) 379–393.
- [18] H.-S. Wang, T.-W. Chou, Transient thermal stress analysis of a rectangular orthotropic slab, *Journal of Composite Materials* 19 (5) (1985) 424–442.
- [19] N. Milošević, M. Raynaud, Analytical solution of transient heat conduction in a two-layer anisotropic cylindrical slab excited superficially by a short laser pulse, *International Journal of Heat and Mass Transfer* 47 (8) (2004) 1627–1641.
- [20] D. W. Hahn, M. N. Ozisik, *Heat conduction*, John Wiley & Sons, 2012.
- [21] H. Wang, T.-W. Chou, Transient thermal behavior of a thermally and elastically orthotropic medium, *AIAA Journal* 24 (4) (1986) 664–672.
- [22] M.-H. Hsieh, C.-C. Ma, Analytical investigations for heat conduction problems in anisotropic thin-layer media with embedded heat sources, *International Journal of Heat and Mass Transfer* 45 (20) (2002) 4117–4132.
- [23] V. Tungikar, K. M. Rao, Three dimensional exact solution of thermal stresses in rectangular composite laminate, *Composite Structures* 27 (4) (1994) 419–430.

- [24] Y. Ootao, Y. Tanigawa, Three-dimensional solution for transient thermal stresses of an orthotropic functionally graded rectangular plate, *Composite structures* 80 (1) (2007) 10–20.
- [25] J. Padovan, Solution of transient temperature fields in laminated anisotropic slabs and cylinders, *International Journal of Engineering Science* 13 (3) (1975) 247–260.
- [26] C. Aviles-Ramos, A. Haji-Sheikh, J. Beck, Exact solution of heat conduction in composite materials and application to inverse problems, *Journal of heat transfer* 120 (3) (1998) 592–599.
- [27] A. A. Delouei, M. Kayhani, M. Norouzi, Exact analytical solution of unsteady axisymmetric conductive heat transfer in cylindrical orthotropic composite laminates, *International Journal of Heat and Mass Transfer* 55 (15) (2012) 4427–4436.
- [28] J. Frankel, M. Keyhani, R. Arimilli, New Orthotropic, Two-Dimensional, Transient Heat-Flux/Temperature Integral Relationship for Half-Space Diffusion, *Journal of Thermophysics and Heat Transfer* 24 (1) (2010) 215–218.
- [29] D. Clements, Thermal stress in an anisotropic elastic half-space, *SIAM Journal on Applied Mathematics* 24 (3) (1973) 332–337.
- [30] J. V. Beck, R. L. McMasters, Solutions for multi-dimensional transient heat conduction with solid body motion, *International Journal of Heat and Mass Transfer* 47 (17) (2004) 3757–3768.
- [31] Y. Chang, R. Tsou, Heat Conduction in an Anisotropic Medium Homogeneous in Cylindrical Regions—Unsteady State, *Journal of Heat Transfer* 99 (1) (1977) 41–46.
- [32] A. Haji-Sheikh, J. Beck, Temperature solution in multi-dimensional multi-layer bodies, *International Journal of Heat and Mass Transfer* 45 (9) (2002) 1865–1877.
- [33] R. J. Marczak, M. Denda, New derivations of the fundamental solution for heat conduction problems in three-dimensional general anisotropic media, *International Journal of Heat and Mass Transfer* 54 (15) (2011) 3605–3612, ISSN 0017-9310.
- [34] K. Poon, R. Tsou, Y. Chang, Solution of anisotropic problems of first class by coordinate-transformation, *Journal of Heat Transfer* 101 (2) (1979) 340–345, ISSN 0022-1481.
- [35] P. Taheri, M. Yazdanpour, M. Bahrami, Analytical assessment of the thermal behavior of nickel–metal hydride batteries during fast charging, *Journal of Power Sources* 245 (2014) 712–720.
- [36] P. Taheri, M. Yazdanpour, M. Bahrami, Transient three-dimensional thermal model for batteries with thin electrodes, *Journal of Power Sources* 243 (2013) 280–289.

- [37] Y.-P. Chang, Analytical solution for heat conduction in anisotropic media in infinite, semi-infinite, and two-plane-bounded regions, *International Journal of Heat and Mass Transfer* 20 (10) (1977) 1019–1028, ISSN 0017-9310.
- [38] C. Truesdell, *Rational Thermodynamics*, Lecture 7 (pp. 365-395), Springer-Verlag, second edn., 1984.
- [39] B. D. Coleman, C. Truesdell, On the reciprocal relations of Onsager, *The Journal of Chemical Physics* 33 (1) (1960) 28–31.
- [40] W. A. Day, M. E. Gurtin, On the symmetry of the conductivity tensor and other restrictions in the nonlinear theory of heat conduction, *Archive for Rational Mechanics and Analysis* 33 (1) (1969) 26–32.
- [41] D. G. Miller, Thermodynamics of irreversible processes. The experimental verification of the Onsager reciprocal relations, *Chemical Reviews* 60 (1) (1960) 15–37.
- [42] J. M. Powers, On the necessity of positive semi-definite conductivity and Onsager reciprocity in modeling heat conduction in anisotropic media, *Transactions of the American Society of Mechanical Engineers* 126 (2004) 670–675.
- [43] J. Wei, Irreversible thermodynamics in engineering, *Industrial & Engineering Chemistry* 58 (10) (1966) 55–60.
- [44] L. Onsager, Reciprocal relations in irreversible processes. II., *Physical Review* 38 (12) (1931) 2265.
- [45] L. Onsager, Reciprocal relations in irreversible processes. I., *Physical Review* 37 (4) (1931) 405.
- [46] G. T. Gilbert, Positive definite matrices and Sylvester’s criterion, *American Mathematical Monthly* (1991) 44–46.
- [47] G. G. Stokes, On the conduction of heat in crystals, *The Cambridge and Dublin Mathematical Journal* 6 (1851) 215–237.
- [48] A. Bendani, A. Dautant, L. Bonpant, Diffusion tensor and molecular jump frequencies in naphthalene single crystals, *Journal de Physique I* 3 (3) (1993) 887–901.
- [49] Z. Xu, J. Travis, W. Breitung, T. Jordan, Verification of a dust transport model against theoretical solutions in multidimensional advection diffusion problems, *Fusion Engineering and Design* 85 (10) (2010) 1935–1940.
- [50] P. J. Roache, Code verification by the method of manufactured solutions, *Journal of Fluids Engineering* 124 (1) (2002) 4–10.
- [51] P. J. Roache, *Verification and Validation in Computational Science and Engineering*, Hermosa, 1998.

- [52] P. Roache, Perspective: a method for uniform reporting of grid refinement studies, *Journal of Fluids Engineering-Transactions of the ASME* 116 (3) (1994) 405–413.
- [53] I. Celik, U. Ghia, P. Roache, C. Freitas, H. Coleman, P. Raad, Procedure for estimation and reporting of uncertainty due to discretization in CFD applications, *Journal of Fluids Engineering* 130 (7) (2008) 078001–078004.